Cement and Concrete Research 42 (2012) 410–423

Contents lists available at SciVerse ScienceDirect

Cement and Concrete Research

journal homepage: http://ees.elsevier.com/CEMCON/default.asp

# Hydration of a low-alkali CEM III/B–$SiO_2$ cement (LAC)

Barbara Lothenbach [a,*], Gwenn Le Saout [a], Mohsen Ben Haha [a], Renato Figi [a], Erich Wieland [b]

[a] Empa, Laboratory for Concrete & Construction Chemistry, CH-8600 Dübendorf, Switzerland
[b] PSI, Laboratory for Waste Management, CH-5232 Villigen PSI, Switzerland

ARTICLE INFO

*Article history:*
Received 6 June 2011
Accepted 11 November 2011

*Keywords:*
Blended cements (D)
Supplementary cementitious material (D)
Thermodynamics (B)
Hydrates (B)
Kinetic (A)

ABSTRACT

The hydration of a low-alkali cement based on CEM III/B blended with 10 wt.% of nanosilica has been studied. The nanosilica reacted within the first days and 90% of the slag reacted within 3.5 years. C-S-H (Ca/Si ~ 1.2, Al/Si ~ 0.12), calcite, hydrotalcite, ettringite and possibly strätlingite were the main hydrates. The pore water composition revealed ten times lower alkali concentrations than in Portland cements. Reducing conditions ($HS^-$) and a pH value of 12.2 were observed. Between 1 month and 3.5 years of hydration more hydrates were formed due to the ongoing slag reaction but no significant differences in the composition of the pore solution or solid phase assemblage were observed.

On the basis of thermodynamic calculations it is predicted that siliceous hydrogarnet could form in the long-term and, in the presence of siliceous hydrogarnet, also thaumasite. Nevertheless, even after 3.5 year hydration, neither siliceous hydrogarnet nor thaumasite have been observed.



## 1. Introduction

The storage of high-level and long-lived radioactive wastes in deep geological repositories is one of the options currently foreseen to ensure long-term safe disposal. A multi-barrier approach has been recommended for the design of a deep geological repository (e.g. [1]). Clay-based host rocks are regarded as hydraulic and chemical barrier to reduce infiltration of water into the near field and to immobilize radioelements in the far field. The clay-based barriers may be locally degraded by the high pH originating from the interstitial water of the cements used for the construction of the cavern (e.g. liner etc.). In ordinary Portland cements pH values of 13.5 or even higher are often observed [2,3]. Cements with a lower pH value of the pore solution would show an improved compatibility with the clay environment and hence reduce local disturbance of the clay-based barrier. Thus, "low-pH" cements have been developed and tested in several national disposal programs [4–6]. The pH value of the interstitial solution of such low-pH cements should optimally be at 11 or lower, and in particular, the high alkalinity caused by the presence of portlandite should be reduced in order to minimize long-term impacts on the clay-based materials. Low-pH values have been obtained in binary mixtures of Portland cement (PC) and silica fume (SF), but also in ternary mixtures with blastfurnace slags or fly ashes [4–7]. In the present study a low-alkali cement "LAC" consisting of 90 wt.% CEM III/B 42.5 L blended with 10 wt.% of nanosilica has been investigated.

The main processes occurring during the hydration of Portland cements are well known (see e.g. the comprehensive book of Taylor [8]). The clinker phases react at various rates and C-S-H,[1] portlandite, ettringite, AFm and hydrotalcite-like phases are formed. The blending of PC with slag or $SiO_2$ leads to a system where the reactions of the Portland cement, of the slag and of $SiO_2$ occur simultaneously with reciprocal influence on the reaction rates [9].

Blending of PC with granulated blastfurnace slags increases the amount of C-S-H formed and lowers the Ca/Si ratio of the C-S-H as slags contain more $SiO_2$ and less CaO than PC. Slags react relatively slowly compared to the PC clinkers in blended systems. The presence of portlandite, C-S-H, ettringite, AFm (monosulfate, monocarbonate), and a hydrotalcite-like phase has been observed experimentally in hydrated PC–slag systems [4,10–16]. At longer hydration times less portlandite (relative to the amount of PC) was found than in PC [4,10,14–18]. Although blastfurnace slags generally contain more $Al_2O_3$ than PC, which could lead to larger amounts of AFm and AFt phases in the PC–slag blends, generally less AFm and AFt phases than in PC have been observed [10,14,15]. The latter finding can be explained with a view to the C-S-H formed in PC–slag blends, which has a lower Ca/Si ratio and a higher Al/Si ratio than in PC [10,13–16,19,20]. Thermodynamic calculations for PC–slag systems showed, in agreement with the experimental observations, the absence of portlandite in blended systems with a high percentage of blast furnace slag, the formation of C-S-H with a lower Ca/Si ratio, the presence of a hydrotalcite-like phase and AFm phases including strätlingite [9,21].

* Corresponding author.
*E-mail address:* barbara.lothenbach@empa.ch (B. Lothenbach).

[1] Cement short hand notation is used: A: $Al_2O_3$; C: CaO; s: $SO_3$; c: $CO_2$; F: $Fe_2O_3$; H: $H_2O$, S: $SiO_2$.

0008-8846/$ – see front matter © 2011 Elsevier Ltd. All rights reserved.
doi:10.1016/j.cemconres.2011.11.008

The addition of slag, silica fume or nanosilica to PC can accelerate the hydration reaction of the PC clinkers [18,22–24] due to the filler effect. The reaction of the silica fume itself causes a reduction in the amount of portlandite formed while larger amounts of C-S-H with a reduced Ca/Si ratio form. Low Ca/Si C-S-H fills up the capillary porosity, which reduces the coarse porosity [25,26] and thus leads to a better durability.

The blending of PC with $SiO_2$ lowers the pH value [11,27–29] as less alkali are present due to the "dilution" of the Portland cement and due to the formation of C-S-H with a lower Ca/Si ratio. Low Ca/Si C-S-H can take up more alkalis [30,31], which reduces the alkali concentration in the pore solution. Hence, the addition of $SiO_2$ lowers the alkali concentration and the pH value more effectively than blending with blastfurnace slag [6,11,32] due to the presence of significantly larger amounts of $SiO_2$.

In the framework of the Cement Clay Interaction (CI) project carried out at the Mont Terri rock laboratory in St. Ursanne, Switzerland, different cements have been emplaced in Opalinus clay (OPA) in 2007 to study their interaction with a clay-based barrier. The temperature in the Mont Terri rock laboratory is 14–15 °C. Complementary to the field experiments the hydration of the cements was studied in detail in laboratory experiments using the same formulations as in the field experiments with the only exception that no sand and gravel were added in order to simplify the sample handling for mineralogical analysis. In this study the composition of the solid and the liquid phase has been investigated for hydration times between 1 h and 3.5 years. Changes in the compositions of the hydrate assemblages and the pore solutions of these cements were determined by X-ray diffraction (XRD), thermogravimetric analysis (TGA), scanning electron microscopy coupled to energy dispersive X-ray spectroscopy (SEM/EDX) and $^{29}$Si-nuclear magnetic resonance (NMR), and by pH measurements, inductively coupled plasma-optical emission spectroscopy (ICP-OES) and ion chromatography (IC) measurements, respectively.

## 2. Materials and methods

### 2.1. Materials

The experiments were carried out using 90 wt.% CEM III/B mixed with 10 wt.% nanosilica and a polycarboxylate based superplasticizer (SP).

The chemical compositions of the materials as given in Table 1 were determined by X-ray fluorescence (XRF). Sulfur and carbonate were determined using a LECO C/S analyzer, and free lime was determined according to Franke [33]. The "total" alkalis were determined with ICP-OES in a solution, which was obtained from digesting 0.20 g of the cements in 20 mL HCl (3%) for several hours [34]. The mineralogical composition of the unhydrated cement was quantified by Rietveld analysis according to the methodology reported elsewhere [35]. TGA measurements indicated the presence of 2.6 wt.% calcite and 1.3 wt.% gypsum. The amorphous amount of the anhydrous sample was estimated using an internal standard. The measured XRF composition of the slag is comparable to the slag composition calculated from the mineralogical composition and the XRF of CEM III/B 42.5 L (Table 1).

The chemical composition of the polycarboxylate superplasticizer was determined by ICP-OES and the content of dissolved organic carbon (DOC) using a Shimadzu TOC-Analyzer. The solid content determined according to EN 480-8 (heating of 2 g superplasticizer for 4 h at 105 °C) was 35 g/100 g.

### 2.2. Hydration experiments

The low-alkali cement (LAC) used in this study was prepared from a CEM III/B (66 wt.% slag, 34 wt.% PC) blended with 10 wt.% nanosilica, which resulted in a mixture of 10 wt.% $SiO_2$, 59 wt.% slag and 31 wt.% PC. Paste experiments were carried out at 20 °C at a water/binder ratio of 1.1, which corresponds to the water/binder ratio used in the Mont Terri field experiments. Due to the presence of the very fine nanosilica neither bleeding nor segregation was observed for any of the LAC pastes. A polycarboxylate based superplasticizer (2.6 g/100 g binder) was added to the mixing water (deionised water). A conduction calorimeter (Thermometric TAM Air) was used for the determination of the rate of hydration heat liberation. A small portion of the mixes was placed in the flasks, capped and placed into the calorimeter at 20 °C.

The composition of the cement pastes was investigated from 1 h to 1310 days of hydration. For each time step individual cement paste samples were prepared. Samples consisting of 1 kg cement and the appropriate amount of water and admixtures were mixed twice for 90 s according to EN 196-3. The pastes were cast in 500 and 100 mL PE-bottles, sealed (to exclude the ingress of $CO_2$) and stored at 20 °C until further use.

**Table 1**
Composition of CEM III/B 42.5 L, nanosilica, superplasticizer (SP) and calculated slag composition.

| | CEM III/B 42.5 L | Slag[a] | (Calculated)[b,c] | Nanosilica[a] | SP |
|---|---|---|---|---|---|
| | | g/100 g | | | |
| CaO | 46.3 | 42.9 | (38.1) | | 0.01 |
| $SiO_2$ | 31.0 | 34.9 | (37.0) | >99.8 | <0.01 |
| $Al_2O_3$ | 10.2 | 11.1 | (13.9) | | 0.01 |
| $Fe_2O_3$ | 1.0 | 0.3 | (0.0) | | <0.01 |
| MgO | 5.8 | 6.7 | (7.7) | | <0.01 |
| $Na_2O$ | 0.26[d] | 0.3 | (0.3) | | 1.5 |
| $K_2O$ | 0.64[d] | 0.4 | (0.6) | | <0.01 |
| $CaO_{free}$ | 0.15 | | | | |
| $SO_3$ | 3.2 | | | | 0.64 |
| S(−II) | | 1.0 | (1.2) | | |
| $TiO_2$[c] | 1.2 | 1.8 | (1.8) | | |
| $Mn_2O_3$[c] | 0.23 | 0.3 | (0.3) | | |
| $CO_2$ | 1.7 | | | | |
| LOI | 0.7 | | | | |
| DOC | 0.009 | | | | 18.3 |
| *Normative phase composition [g/100 g]* | | | | | |
| Amorphous | 65.9 | | | | |
| Alite | 16.7 | | | | |
| Belite | 5.6 | | | | |
| Aluminate | 0.9 | | | | |
| Ferrite | 3.4 | | | | |
| $CaO_{free}$ | 0.15 | | | | |
| Periclase | 0.3 | | | | |
| $CaCO_3$ | 3.9 | | | | |
| Dolomite | 0.7 | | | | |
| Gypsum | 2.2 | | | | |
| Syngenite | 0.30 | | | | |
| $K_2SO_4$[e] | 0.30 | | | | |
| $Na_2SO_4$[e] | 0.05 | | | | |
| Present as solid solution in the clinker phases | | | | | |
| $K_2O$[f] | 0.06 | | | | |
| $Na_2O$[f] | 0.03 | | | | |
| MgO[f] | 0.27 | | | | |
| Density [kg/dm$^3$] | 2.94 | 2.2 | | | |
| Surface [m$^2$/g] | 0.442 | | | 200 | |
| Primary particle size | | | | 12 nm | |

[a] Data from producer.
[b] For comparison a theoretical slag composition was calculated from the measured XRF data and the mineralogical composition of the CEM III/B 42.5
[c] Not considered for modeling.
[d] The "total" alkalis were determined with ICP-OES in a solution, which was obtained by digesting 0.20 g of the cements in 20 mL HCl (3%) for several hours [34]. The total alkali contents determined by this method are somewhat higher than the XRF results ($Na_2O = 0.21$, $K_2O = 0.34$).
[e] Readily soluble alkalis calculated from the concentrations of alkalis measured in the solution after 5 min agitation at a w/c of 10; present as alkali sulfates.
[f] Calculated based on the chemical analysis and the mineralogical composition.

*2.2.1. Analysis of solid phases*

After appropriate hydration times, a small disk was cut from the single 100 mL paste samples, crushed, washed in acetone to stop the hydration process, dried for 2 days at 40 °C and manually ground and sieved to obtain particles with diameter <63 μm. The crushed material was used for XRD (first day only), TGA, and NMR measurements and to determine the amount of slag reacted by selective dissolution. After the first day, when the pastes had been sufficiently hardened, XRD measurements were carried out on solid samples cut from the 100 mL bottles, immediately after cutting.

A Mettler Toledo TGA/SDTA 8513 was used for TGA measurements. Samples of approx. 10 mg crushed material were heated under a nitrogen atmosphere at 20 °C/min from 30 to 980 °C. The amount of bound water in the pastes was calculated after exchange with isopropanol and drying at 40 °C from the total water loss up to 600 °C. The amount of portlandite and calcite was estimated from the weight loss between 400–520 °C and 600–700 °C, respectively. The weight losses between 50–110 °C and 110–140 °C are indicative for the amount of ettringite and gypsum. Quantification of gypsum and especially ettringite by TGA is hampered due to the dominant water loss of C-S-H in the temperature range from 50 to 250 °C. Thus, only gypsum was quantified as, at early hydration times, little C-S-H is present.

X-ray diffraction data were collected using a PANalytical X'Pert Pro MPD diffractometer in a 2θ–θ configuration employing the $CuK_\alpha$ radiation ($\lambda = 1.54$ Å) with a fixed divergence slit size 0.5° and a rotating sample stage. The samples were scanned between 5 and 70° with the X'Celerator detector. To verify whether (siliceous) hydrogarnet was present in the samples hydrated for 3.5 years, selective extractions with salicylic acid and methanol (SAM) were carried out. To this aim 20 g salicylic acid was mixed with about 300 mL methanol. Five grams of dried cement paste was added. The suspension was mixed for about 2 h using a magnetic stirrer. After sedimentation of the solid material, the supernatant solution was decanted and the wet paste was filtrated using a 0.45 μm nylon Whatman filter and a Buchner funnel. The filtrate was dried at 40 °C prior to XRD analysis. The aim of this extraction was to minimize overlapping diffraction peaks from the silicates and to increase the peak intensities of the remaining phases. Alite, belite, C-S-H, portlandite and ettringite dissolve while aluminate, ferrite and also siliceous (Si-) hydrogarnet [36,37] remain in the residue amenable to further analysis.

The $^{29}Si$ NMR measurements were performed at room temperature using a Bruker Avance 400 NMR spectrometer with a 7 mm CP/MAS probe. The $^{29}Si$ MAS NMR single pulse experiments were recorded at 79.49 MHz using the following parameters: 4800 Hz spinning speed, 2048 scans, 45° pulses of 3 μs, 30 s relaxation delays, RF field strengths of 41.6 kHz during TPPM decoupling sequence. The chemical shifts of the $^{29}Si$ MAS NMR spectra were referenced to an external sample of tetramethylsilane (TMS). The observed $^{29}Si$ resonances were analyzed using the $Q^n$(mAl) classification, where a Si tetrahedron is connected to n Si tetrahedral with n varying from 0 to 4 and m is the number of neighboring $AlO_4$ tetrahedra. The amount of nanosilica or silica fume, respectively, was determined based on the amount of Si associated with the $Q^4$ peak at −110 ppm. The latter amount was obtained by non-linear least-square fits of the regions of interest using the software "DMFIT" developed by Massiot et al. [38].

The SEM/EDX investigations were carried out on samples, which had been dried at 40 °C, pressure impregnated with epoxy resin, polished and carbon coated. Polished samples were examined with an environmental scanning electron microscopy (Philips ESEM FEG XL 30) using backscattered secondary electron (BSE) images and energy dispersive X-ray spectroscopy (EDX) analysis. BSE image analysis (SEM-IA) was used to determine the amount of unreacted slag as well as the amount of coarse porosity (>0.1 μm) after 1 and 3.5 years hydration. The technique uses the gray level histogram and morphological segmentation to determine the different solids observed in a BSE image [39–41]. The gray level in the backscattered electron images depends on the average atomic number of the examined area. Thus, unreacted slag appears in the brightest contrast, hydrates appear in gray or darker color and the pores appear black. The reaction of the anhydrous slag was determined by comparing the volume of anhydrous slag in the hydrated pastes with the volume of the slag content in the unhydrated paste. The uncertainty, based on the threshold and edge detection as well as the effect of presence of air pores within the mixes, was estimated to be about 2–3%. The volume of coarser pores as determined by SEM-IA includes pore sizes in the range from 0.1 to 5 μm depending on the magnification (2500×) used. The error in the case of porosity measurements was lower since it includes only the threshold errors, which ranges from 0.5 to 1%.

The degree of reaction of the slag was also estimated by selective dissolution of the unhydrated and hydrated LAC using a mixture of EDTA and triethanolamine according to the procedure suggested by Lumley et al. [42]. This mixture should allow selective dissolution of the unreacted clinker, gypsum and the hydration products, except hydrotalcite, while the slag should not be affected. For each hydration age, 0.50 g of dried powder (dried for 2 days at 40 °C and manually ground to <63 μm as described above) was diluted in the EDTA solution, stirred for 2 h and filtered through a 90 mm diameter Whatman GF/C filter. The residue was washed 5 times with 10 mL of distilled water and dried at 105 °C for 1 h before weighing. The amount of slag reacted was then calculated by comparison of the residues determined for the unhydrated and the hydrated samples. Lumley et al. [42] recommended a correction taking into account the amount of hydrotalcite by assuming that all the MgO from the amorphous part of the reacted slag converts to a hydrotalcite-like phase.

*2.2.2. Analysis of pore solutions*

During the first day of hydration pore solutions were collected by vacuum filtration or pressure filtration. After one day and longer, pore fluids of the hardened samples were extracted from the 500 mL samples using the steel die method and pressures up to 530 N/mm$^2$. In all cases, the solutions were immediately filtered using 0.45 μm nylon filters. 5 mL aliquots were diluted with 20 mL Milli-Q water and acidified with 0.2 mL concentrated $HNO_3$ to prevent precipitation of solid phases. These samples were analyzed using ICP-OES. Additionally, 10 mL aliquots were sampled in glass vials for DOC measurements using the Shimadzu TOC-WP® analyzer. Finally, pH measurements were carried out immediately after filtration using small aliquots of the pore solution. pH was measured using a Knick pH meter (pH-Meter 766) equipped with a Knick SE100 electrode. The pH electrode was calibrated against KOH solutions of known concentrations.

Reduced sulfur species cannot be determined in acidified samples as volatile $H_2S$ and $H_2SO_3$ ($= SO_2 + H_2O$) form in the presence of acid. Thus, the concentration of total sulfur was determined by ICP-OES in the alkaline solutions. The concentrations of $SO_4^{2-}$, $SO_3^{2-}$ and $S_2O_3^{2-}$ were obtained after stabilization in 0.0035% formaldehyde solutions using IC (Metrohm Compact IC 761). Sulfide, $HS^-$, was stabilized with Zn-acetate (for details see Gruskovnjak et al. [43]) and measured by colorimetry. All sulfur measurements were carried out within one day after sampling and each sample was analyzed at several sample dilutions using Milli-Q water.

*2.3. Thermodynamic modeling*

Thermodynamic modeling was carried out using the Gibbs free energy minimization program GEMS [44,45]. GEMS is a geochemical modeling code which computes equilibrium speciation of the dissolved species as well as the kind and amount of solids precipitated. Chemical interactions involving solids, solid solutions, aqueous electrolyte and gas phase are considered simultaneously. The thermodynamic data for aqueous species as well as for many solids were

taken from the PSI-GEMS thermodynamic database [46,47], while the solubility products for cement minerals were taken from the cemdata07 database [48–50]. The cemdata2007 dataset includes thermodynamic data of common cement minerals such as C-S-H, different AFt and AFm phases, hydrotalcite and hydrogarnets. No restrictions on the kind of hydrates calculated were imposed, with the exception of siliceous hydrogarnet ($C_3AS_{0.8}H_{4.4}$), whose formation was suppressed as its formation seems to be kinetically hindered at ambient temperature [48]. For modeling purposes, the formation of ideal solid solutions between Al- and Fe-containing analogues was assumed [48]. Thus, the expressions ettringite, monocarbonate, monosulfate, hemicarbonate or hydrotalcite in this paper also refer to the solid solutions between the Al- and Fe-containing analogues. The solid solution formation between ettringite and thaumasite [51] was not included in the calculations, as no such solid solution model is currently available.

As slag is present in the mixture, the formation of FeS (troilite) was taken into account. In addition, also thermodynamic data for disordered FeS (mackinawite) were added to the database (Table 2). The formation of pyrite ($FeS_2$) was suppressed in the calculations for kinetic reasons. Furthermore, it was assumed that no $O_2$ would ingress during the experiment.

Due to its variable composition, the C-S-H phase was modeled using a solid solution model with the end-members jennite $(CaO)_{1.67}(SiO_2)_1\cdot(H_2O)_{2.1}$ and tobermorite $(CaO)_{0.83}(SiO_2)_1\cdot(H_2O)_{1.3}$. The model was originally developed by Kulik and Kersten [52,53] and later adapted by Lothenbach et al. [48]. The uptake of aluminum by C-S-H was simply taken into account by using the measured Al/Si ratios (=0.12) in the C-S-H as thermodynamic models allowing the Al-uptake by C-S-H to be calculated are not available. It was assumed that the incorporation of aluminum, which occurs mainly at bridging sites of the C-S-H [54–56], does not increase the molar volume of the tobermorite-like C-S-H but stabilizes the tobermorite distance at 14 Å [55]. The uptake of alkalis by C-S-H was estimated by using an ideal solid solution model between jennite-, tobermorite-like C-S-H and $[(KOH)_{2.5}\ SiO_2\ H_2O]_{0.2}$ and $[(NaOH)_{2.5}\ SiO_2\ H_2O]_{0.2}$ as proposed by Kulik et al. [57]. Using the experimental data of Hong and Glasser [30], $\Delta_fG°$ values could be fitted for $[(KOH)_{2.5}\ SiO_2\ H_2O]_{0.2}$ and $[(NaOH)_{2.5}\ SiO_2\ H_2O]_{0.2}$ (see Table 2).

## 3. Experimental results

### 3.1. Heat of hydration

Isothermal conduction calorimetry (Fig. 1) of the LAC showed two main hydration peaks after 2 and 10 h and a broad hydration peak

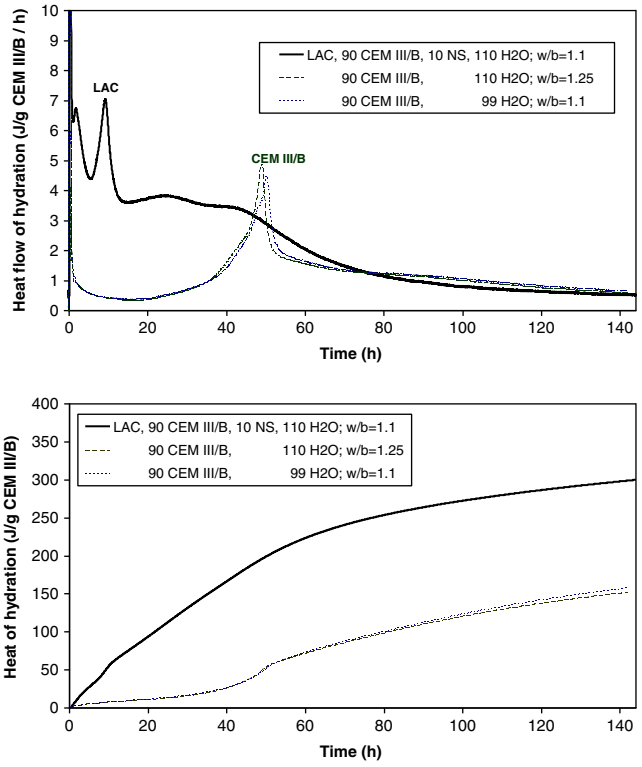


**Fig. 1.** Heat flow development and cumulative heat of hydration of LAC paste and CEM III/B (LAC without nanosilica (NS)). Data refer to g of CEM III/B without nanosilica.

was visible up to a hydration time of 80 h. If the same CEM III/B was hydrated in the absence of nanosilica a double peak after approx. 50 h was observed as well as a significantly lower heat of hydration (independently whether the water to cement (w/c) or the water to binder (w/b) ratio was kept constant). Bleeding was observed for the two CEM III/B samples, but not for the LAC paste containing 10 wt.% of nanosilica. Although only 10 wt.% of nanosilica was intermixed, its presence increased considerably the heat of hydration during the first days. The intermixing of fine materials is known to accelerate early hydration as fine materials offer additional surface area for nucleation and precipitation of solids. Several authors observed an acceleration of the hydration of PC in the presence of microsilica [22–24,60], especially at higher w/b ratios. However, after one month or longer, the difference in the degree of reaction of the Portland cement clinkers was found to be small [24,60]. In addition to the acceleration of the PC hydration (as visible by the shift of the two main peaks from 50 to 2 and 10 h), also a significant increase in the total heat of hydration was observed, which can be attributed to the fast reaction of the 10 wt.% nanosilica to form C-S-H. Si-NMR measurements (see below) showed that most of the nanosilica had reacted within the first 2–3 days, which is supported by the disappearance of the broad peak after 70 h (LAC in Fig. 1). The first peak of LAC hydration after 2 h might be related to the strong reaction of alite during the first hours (see XRD and TGA data presented in Section 3.3), while the second peak after 10 h coincides with the depletion of the sulfate carrier.

### 3.2. Dissolution of slag and nanosilica

#### 3.2.1. Slag

While the progress of reaction of the clinker phases can be followed by XRD (see below), this is neither possible for the nanosilica nor for the slag as both are X-ray amorphous. Hence, the degree of slag reaction was estimated (i) by selective dissolution and (ii) by image analysis.

**Table 2**
Thermodynamic data (25 °C, 1 bar) used in addition to the data given in the PSI-GEMS [46,47] and the cemdata07 database [48–50].

| Reaction | log K | $\Delta_fG°$ [kJ/mol] | Reference |
|---|---|---|---|
| *Solids* | | | |
| $FeS(mackinawite)+2H^+ \Leftrightarrow Fe^{2+}+H_2S(aq)$ | −4.87 | −91.6 | [58] |
| $C_3FS_{0.8}H_{4.4}$[a] $\Leftrightarrow 3Ca^{2+}+2Fe(OH)_4^-+0.8HSiO_3^-+3.2OH^-+0.4H_2O$ | −34.19 | −4474.2 | This paper |
| $[(KOH)_{2.5}\ SiO_2\ H_2O]_{0.2}$ | | −440.8 | Fitted from [30] |
| $[(NaOH)_{2.5}\ SiO_2\ H_2O]_{0.2}$ | | −431.2 | Fitted from [30] |
| *Aqueous complexes* | | | |
| $FeSH^+$ $FeS(s)+H^+ \Leftrightarrow FeSH^+$ | 2.05 | −103.3 | [58] |
| $Fe(SH)_2^0$ (aq) $FeS(s)+H_2S(aq) \Leftrightarrow Fe(SH)_2^0$ (aq) | −3.43 | −99.99 | [58] |

[a] The solubility of $C_3FS_{0.8}H_{4.4}$ was estimated to be $10^{-4.32}$ log units lower than the solubility product of $C_3AS_{0.8}H_{4.4}$ ($10^{-29.87}$ [49]) as suggested by Babushkin [59], for details see [48]. $C_3FS_{0.8}H_{4.4}$ and $C_3AS_{0.8}H_{4.4}$ were excluded from most calculations for kinetic reasons (see text).

*Selective dissolution* techniques allow preferential dissolution of the hydration products, the unreacted clinker and gypsum, while the slag should be much less affected by this procedure. The percentage of slag reacted ($x$) is obtained by comparing the residues determined after the selective dissolution by EDTA of the unhydrated ($r_u$) and the hydrated samples ($r_{HP}$) according to:

$$x = \%\,slag\,reacted = 100\frac{R_u - R_{HP}}{R_u} = 100\frac{0.38 - R_{HP}}{0.38} \quad (1)$$

where $R_u$ and $R_{HP}$ are the residues of the unhydrated and the hydrated samples corrected for the amount of bound water ($w_b$):

$$R_u = \frac{r_u}{1 - w_{b,u}};\; R_{HP} = \frac{r_{HP}}{1 - w_{b,HP}}. \quad (2)$$

The data indicate a fast dissolution of the slag during the first days, which proceeded at a lower rate after 1 week (Fig. 2 and Table 3). After 3.5 years 20% of the slag present has not yet reacted.

Lumley et al. [42] suggested to correct the undissolved fraction for the formation of hydrotalcite (which is not dissolved by the EDTA procedure) according to

$$x_{ht} = 100\frac{0.38 - (R_{HP} - 0.38hMx_{ht})}{0.38}. \quad (3)$$

The expression $0.38hMx_{ht}$ equals to the mass of hydrotalcite formed from the reacted slag, with $h = 2.35$ (= mass of dried hydrotalcite in g) formed from 1 g of MgO in the slag [42] and $M = 0.067$ (= MgO content of the slag). Rearranging Eq. (3) results in

$$x_{ht} = 100\frac{R_u - R_{HP}}{R_u * (1 - hM)} = 100\frac{0.38 - R_{HP}}{0.38 * (1 - 2.35 * 0.067)}. \quad (4)$$

If this correction is applied more slag is calculated to have reacted and only 10% of the slag remained unreacted after 3.5 years of hydration.

*Image analysis (SEM-IA)* allows the reaction of the slag to be determined based on a comparison of the volume of the remaining anhydrous slag in the hydrated pastes with the volume of the slag originally present in unhydrated paste. Based on SEM-IA the fraction of slag reacted in LAC was 89% after 1 year and 92% after 3.5 years (Fig. 2, Table 3).

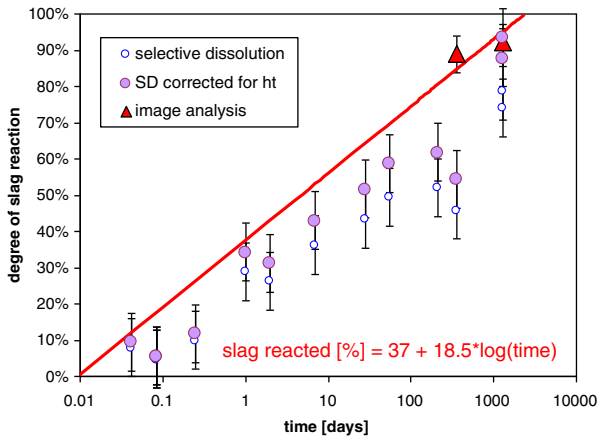


**Fig. 2.** Reaction of slag as a function of hydration time determined by selective dissolution (SD) (with and without correction for the presence of hydrotalcite (ht)) and by image analysis.

**Table 3**
Measured amount of unreacted slag by selective dissolution technique and by image analysis in LAC as function of time. The amount of nanosilica was determined by Si-NMR.

| Time [days] | Bound water $w_b$[a] [g/100 g] | Residue[b] r [g] | Slag reacted[e] [%] | Corr. for ht[f] [%] | Porosity[c] | Unreacted nanosilica[d] [g/100 g] [wt.%] |
|---|---|---|---|---|---|---|
| 0 | 0.9 | 0.38 | 0 | 0 | | 9.6 |
| 0.04 | 3.6 | 0.34 | 8.0 | 9.4 | | 9.9 |
| 0.08 | 4.1 | 0.35 | 4.7 | 5.6 | | – |
| 0.08 | 4.1 | 0.35 | 4.7 | 5.6 | | – |
| 0.25 | 4.4 | 0.33 | 10.0 | 12 | | 10.6 |
| 1 | 8.3 | 0.25 | 29 | 34 | | 7.5 |
| 2 | 11.5 | 0.25 | 26 | 31 | | 1.7 |
| 7 | 14.1 | 0.21 | 36 | 43 | | 0.9 |
| 28 | 16.9 | 0.18 | 43 | 52 | | – |
| 56 | 17.4 | 0.16 | 49 | 59 | | 0.7 |
| 210 | 18.4 | 0.15 | 52 | 62 | | – |
| 356 | 18.1 | 0.17 | 46 | 54 | | 0.0 |
| 1310 | 19.5 | 0.07 | 79 | 94 | | 0.0 |
| 1310 | 19.9 | 0.08 | 74 | 88 | | 0.0 |
| *Image analysis* | | | | | | |
| 356 | | | | 89 | 13.7 | |
| 1310 | | | | 92 | 11.7 | |

[a] The bound water content ($w_b$) was determined from the weight loss between 40 and 600 °C measured by TGA.
[b] A total of 0.5 g of LAC was used. The residue of CEM III/B is 0.35, of $SiO_2$ is 0.47.
[c] The porosity derived from BSE images underestimates the total porosity as only the coarser pores (0.1–5 μm) are visible.
[d] The amount of nanosilica (NS) is determined by Si-NMR.
[e] Not corrected for the presence of hydrotalcite.
[f] Corrected for the presence of hydrotalcite according to Lumley et al. [42]: 1-2.35 * fraction MgO.

Comparison of the results from SEM-IA and the selective dissolution technique indicates a higher degree of slag reaction by SEM-IA (Fig. 2, Table 3). The selective dissolution technique, without correction for the presence of hydrotalcite, strongly underestimates the degree of slag reaction, as a portion of the hydrates is not dissolved. An amorphous residue rich in Mg, Al and Si hydroxides and carbonates is still present after selective dissolution with EDTA [10,40,42,61–64]. Consideration of a correction factor based on the MgO content of the slag and the fraction of slag reacted [42], suggests a higher degree of slag reaction. Note, however, some portion of the PC is often not dissolved by the selective dissolution techniques [10,40,64], while a part of the unhydrated slag is dissolved [10,63,64]. If the slag and the PC can be measured separately, correction factors can be applied, but it is uncertain how the reaction of the fine fraction of the slag will affect the fraction of slag dissolved in the EDTA test at longer hydration times. Based on the number of corrections and the uncertainty associated with them, it is believed that the selective dissolution method is not reliable. This agrees with previous findings for slag systems [63,65], for PC–slag [10,64] and for PC–fly ash systems [40].

Image analysis indicates that after 1 year and longer approximately 90% of the slag present has reacted. This is a somewhat higher degree of reaction than reported for other PC–slag systems: ~70% (20 years, Si-NMR [15]), ~75% (2 years, SEM-IA [10,64]). The higher reaction degree is probably due to the large amount of water available in the experiments presented here. In this study a water/binder ratio of 1.1 was used, while in the other studies water/binder ratios of 0.4 and 0.5 had been used [10,15,64].

### 3.2.2. Nanosilica

The reaction of the nanosilica was determined by $^{29}Si$ NMR. The Si NMR spectra of the cement and the slag show a very broad peak (Fig. 3) including the $Q^0$ signals of alite and belite at around −70 ppm and the $Q^0$ to $Q^3$ signal of the slag (−60 to −90 ppm).

The broad $Q^4$ peak at −110 ppm is characteristic for amorphous silica. After 1 year of hydration, the alite and belite peaks have

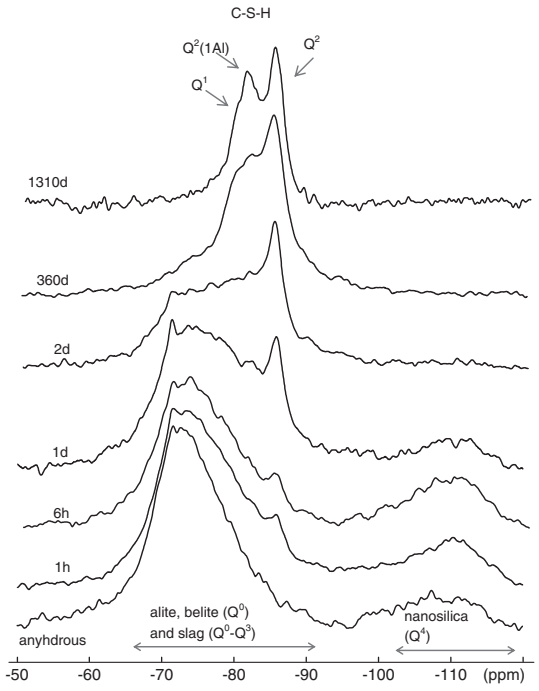


**Fig. 3.** $^{29}$Si MAS NMR spectra of hydrating LAC.

disappeared and the amount of slag is largely reduced. As previously shown in blended cements [62] and alkali activated slags [65,66], the spectra contain at least three resonances from C-S-H at around −78, −81 and −84 ppm, respectively assigned to $Q^1$, $Q^2$(1Al) and $Q^2$ species. The overlap of the peaks does not permit an unambiguous deconvolution between alite, belite, slag and C-S-H. The large amount of $Q^2$ at 1310 days reflects the longer mean chain length of the C-S-(A)-H and higher substitution of Si by Al compared to C-S-H in OPC (see [36,67] and references therein). Already after 1 h, the formation of C-S-H is visible from the $Q^2$ peak at −84 ppm in Fig. 3.

The reactivity of nanosilica and silica fume is generally larger than the reactivity of slag or fly ash [18] due to their small particle size. The amount of nanosilica reacted was calculated based on the amount of silicon associated with the $Q^4$ peak at −110 ppm compared to the amount of amorphous silicon in the anhydrous LAC. After two days of hydration, 80% of the nanosilica had reacted and 90% after 7 days (Table 3, Fig. 4). The $^{29}$Si NMR indicates little reaction of the nanosilica during the first day, while the calorimetric data (Fig. 1) and the complete absence of portlandite in all samples indicate a significant reaction of the nanosilica during the first hours. The analytical error associated with the quantitative determination of 10% nanosilica in the blend is considerable, which could be reason for this apparent non reaction of the nanosilica during the first hours.

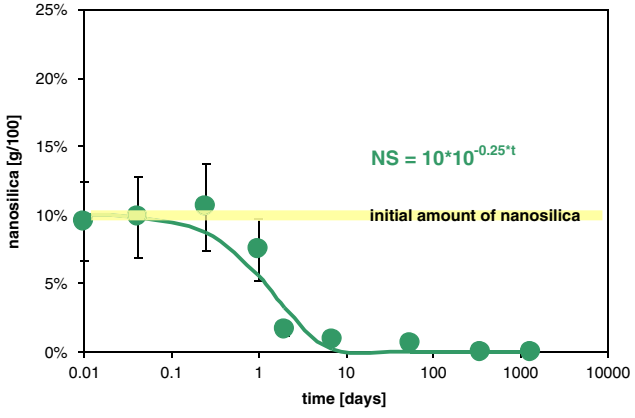


**Fig. 4.** Reaction of the nanosilica as a function of hydration time determined by Si-NMR. Error ± 30% of measured value.

### 3.3. Hydrates

#### 3.3.1. XRD and TGA

In accordance with the low PC content (31 wt.%), the XRD and TGA data of the unhydrated LAC show only a moderate amount of clinker and gypsum (Figs. 5 and 6). The slag gives rise to an inconspicuous increase of the baseline in XRD between 26 and 33 °2 theta. Gypsum disappeared within 1 day hydration, while the clinker phases reacted almost completely within 1 week. The main hydration products identified by XRD and TGA are ettringite and tobermorite-like C-S-H. Already after 1 h the formation of C-S-H is indicated in the TGA data by the broad peak of water loss between 50 and 250 °C (Fig. 6) and by the presence of a peak at −84 ppm in Si NMR (Fig. 3). This observation of early C-S-H formation is consistent with the observed reaction of alite during the first hour (see XRD data in Fig. 5) and with the first main heat development observed after 1 to 2 h in the calorimetric data for LAC (Fig. 1). Even though a fast reaction of alite was observed, portlandite was not observed any time during hydration, neither by TGA nor by XRD.

In addition to the major phases, between 1 day and 1 year a minor peak at 10.8 °2 theta is visible in the XRD indicating the presence of some hemicarbonate. After 3.5 years of hydration, however, hemicarbonate was not detectable by XRD anymore. TGA indicates also the presence of hydrotalcite (weight loss at around 400 °C [68]), while XRD gives no clear indication whether or not hydrotalcite (main peak at 11.5 °2 theta) formed. The XRD data show that only ettringite but no thaumasite had formed. The XRD and TGA data indicate no significant changes in the composition of the phase assemblage (C-S-H, ettringite, possibly hydrotalcite and AFm phases) during hydration but mainly an increase in bound water due to the formation of increasing amounts of hydrates (Table 3, Fig. 6). The main difference between the LAC and a PC is the complete absence of portlandite and the presence of C-S-H with a lower Ca/Si ratio.

Neither strätlingite (main peak at 7.0 °2 theta), nor thaumasite (main peak at 9.2 °2 theta) nor Si-hydrogarnet (28.9 and 32.4 °2 theta), whose possible formation was indicated from the saturation index (see below) and thermodynamic modeling, could be identified by XRD. To verify whether or not Si-hydrogarnet (katoite) was present, a selective extraction with salicylic acid and methanol (SAM) was carried out. The aim of this extraction is to reduce overlaps in the diffraction peaks and to increase the peak intensities of the remaining phases. Alite, belite, C-S-H, portlandite and ettringite are dissolved while aluminate, ferrite and Si-hydrogarnet remain in the residue and can be detected [36,37]. Even after SAM extraction, no Si-hydrogarnet was observed after 3.5 years of hydration, only calcite, dolomite and quartz could be clearly identified. In contrast, Al/Fe-

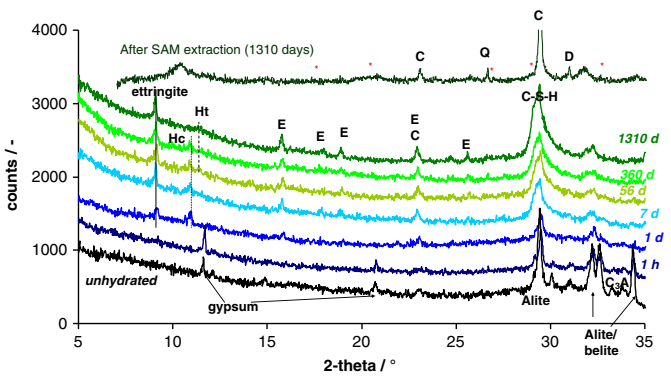


**Fig. 5.** XRD of the hydrating LAC paste and of the residue after SAM extraction. C: calcite, D: dolomite, E: ettringite, Q: quartz. *Main peaks of Si-hydrogarnet (katoite).

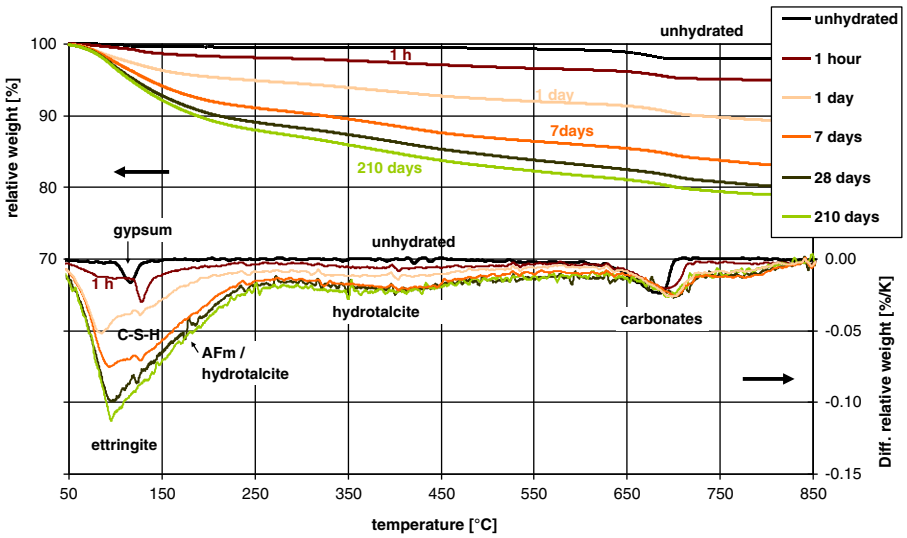


**Fig. 6.** TGA/DTG of the hydrating LAC paste.

containing Si-hydrogarnet has been observed in aged Portland cements [37,69–73]. Experimental evidence suggests that Si-hydrogarnet only forms at room temperature if both Al(III) and Fe(III) are present [73]. The lower pH and the predominance of reducing conditions are expected to lead to very low dissolved Fe(III) concentrations such that the formation of Fe-containing Si-hydrogarnet seems unlikely.

### 3.3.2. Microstructure

The SEM/BSE images taken from the surface of the polished LAC samples hydrated for 1 and 3.5 years show the presence of small amounts of unhydrated slag particles. A hydration rim was observed around some slag grains (Fig. 7). Even though a high w/b of 1.1 was used a dense microstructure developed with relatively little coarse porosity (black areas) of 12 vol.% after 3.5 years (Table 3). The dense matrix also gave rise to the formation of some cracks.

SEM/EDX analysis resulted in a mean Ca/Si molar ratio of $1.1 \pm 0.2$ after 1 year and $1.2 \pm 0.2$ after 3.5 year and at both times a Ca/(Si + Al) molar ratio of $1.05 \pm 0.2$. The clear correlation of the Mg/Si versus the Al/Si ratio in the EDX indicates the presence of a hydrotalcite-like phase with a Mg/Al molar ratio of 1.6–1.7. The abscissa indicates an Al/Si molar ratio in C-S-H of 0.12 to 0.14 with no significant change between 1 and 3.5 years (Fig. 8).

## 3.4. Pore solutions

### 3.4.1. Measured concentrations

During the first 6 h the pore solution of LAC was dominated by potassium, sulfate, hydroxide, sodium and calcium (Fig. 9, Table 4); similar to the compositions of pore solutions of Portland cements (e.g. [2,37,74,75]). As for PC, the high concentrations of K, Na, Ca, sulfate and hydroxide present after 1 h were due to the fast dissolution of calcium- and alkali-sulfates. After 8 h and longer, the calcium and sulfate concentrations were strongly reduced as the calcium sulfate carrier was exhausted. After 1 day minimal sulfate (0.1 mM) and calcium (7 mM) concentrations were observed in the pore solution. These values are in the range of calcium and sulfate concentrations reported for Portland cements [2,37,72,74,75]. Up to 1 day alkali and hydroxide concentrations continued to increase as the reaction of the PC released alkalis to the pore solution while at the same time water was consumed.

After the first day, however, alkali and hydroxide concentrations started to drop, indicating an increasing uptake of alkalis by the hydrates. The observed high uptake of alkalis can be attributed to the formation of a C-S-H with a low Ca/Si ratio, as the uptake of alkalis by C-S-H increases with decreasing Ca/Si ratio [30,31]. Somewhat higher Al and Mg concentrations (Table 4) were observed in the LAC than in Portland cements (Al<0.1 mM and Mg<0.001 mM [2,37,72,75,76]). The measured Fe concentration of about 0.01 mM was significantly higher than that observed in the pore solutions of

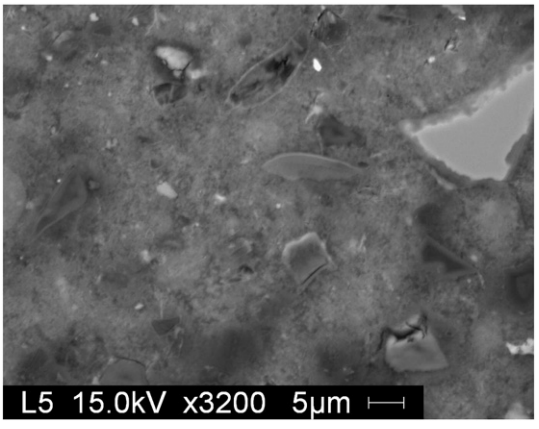


**Fig. 7.** SEM/BSE image of the polished LAC sample hydrated for 3.5 years.

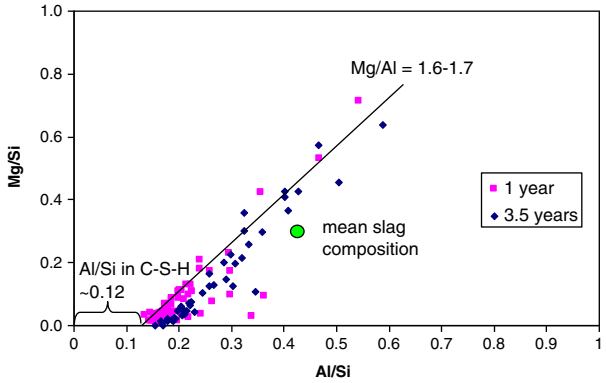


**Fig. 8.** Atomic Mg/Si and Al/Si ratio of hydrated LAC pastes determined using EDX analyses on polished surfaces.

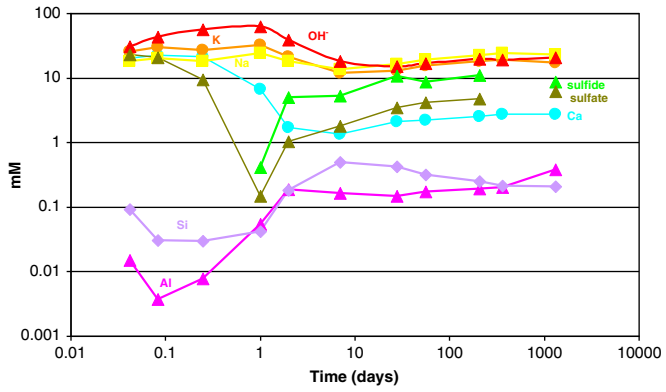


**Fig. 9.** Measured composition of the pore solution as a function of hydration time.

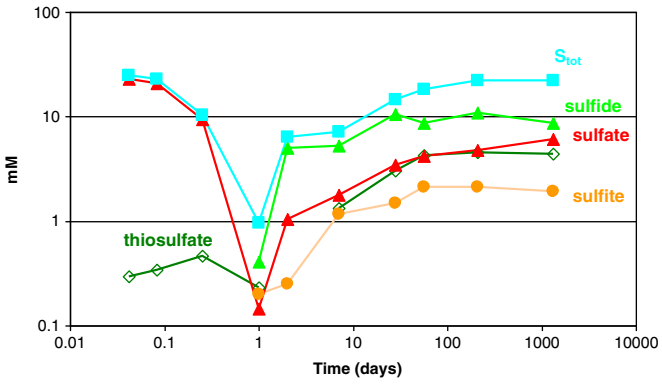


**Fig. 10.** Measured sulfur species in the pore solution as a function of hydration time.

Portland cements (<0.001 mM) [3,37,72]. The relatively high Fe concentrations might be caused by the presence of reducing conditions in the presence of slag. Under reducing conditions Fe(+II) is favored over Fe(+III) and Fe(+II) is more soluble than Fe(+III) under alkaline conditions. After the first week, the composition of the pore solution remained more or less constant even though the slag continuously reacted (see Fig. 2).

Sulfide originating from the dissolution of the slag could first be detected after 1 day (Fig. 10, Table 5). The sulfide concentration increased strongly during the first month of reaction and remained rather constant thereafter. Also the dissolved sulfate concentration increased significantly between 1 day and 1 month, probably due to the oxidation of sulfide originating from the reaction of the slag. The presence of about 20 mM of negatively charged sulfur species reduced the concentration of hydroxides in the pore solutions, thus lowering the pH. The steep increase in the $HS^-$ concentration during the first two days indicates a significant reaction of the slag in this period of time followed by a much slower reaction afterwards. This agrees well with the reactivity of the slag as observed by the EDTA extraction method (Fig. 2, Table 3). At later ages, however, the $HS^-$ concentration is not directly related to slag dissolution as the oxidation to sulfate and possibly the uptake by solids [79] are more important [63,80]. In addition to sulfide (from the slag) and sulfate, $SO_4^{2-}$ (originating from PC), also thiosulfate $S_2O_3^{2-}$ and sulfite $SO_3^{2-}$ were observed in the pore solution of the LAC. During the oxidation of $HS^-$ to $SO_4^{2-}$, the intermediates $S_2O_3^{2-}$ and $SO_3^{2-}$ formed. The oxidation of $S_2O_3^{2-}$ is slow at higher pH values as the presence of sulfide seems to inhibit further oxidation of sulfite [77,78]. Thus, $S_2O_3^{2-}$ and $SO_3^{2-}$ were present as intermediate products in the pore solution (Table 5). Based on the measured pH values, sulfide, thiosulfate, sulfite and sulfate concentrations (cf. Tables 4 and 5) a redox potential $E_H$ of about −0.57 V was calculated for the LAC at later hydration times. The presence of sulfide, thiosulfate and sulfite and the predominance of reducing conditions in the PC–slag blend agrees with earlier experimental findings in such blends [29,79,81,82]. In alkali activated or supersulfated slags even more strongly reducing conditions have been observed as indicated by the higher sulfide/sulfate ratio in the pore solution [43,63,80,83]. It is expected that the predominance of reducing conditions also has an influence on the redox state of other redox sensitive elements such as Fe, Mo, Cr and Mn present in the cement and the pore solution.

Dissolved organic carbon (DOC; from the polycarboxylate (PCE) based superplasticizers) was found to be already strongly reduced after 1 h as approximately 90% of the superplasticizer was sorbed onto, or coprecipitated with the newly formed solids (Table 4). After 28 days of hydration, 40–50 mM DOC was still in the pore solution (the original mixing solution had contained 370 mM DOC). At longer hydration time, a very moderate increase in the DOC concentration to 60 mM was observed as the amount of pore solution present decreased. The observed DOC concentrations after 28 days and longer are comparable to the concentrations observed in the pore solution of a Portland cement (40 to 70 mM) [84,85], where a somewhat lower amount of the same superplasticizer had been used. In a study where another type of PCE based superplasticizers had been used in a similar concentration, a lower uptake of SP by the solids was observed and 100 to 160 mM of DOC was still dissolved in the pore solution after 1 day and longer [86]. This indicates that the

**Table 4**
Measured total concentrations in the pore solutions.

| Age [days] | Al | Ba | Ca | Cr | Fe | K [mM] | Mg | Mo | Na | Si | Sr | DOC[a] | $OH^{-}$[b] | pH– | cb[c] [%] |
|---|---|---|---|---|---|---|---|---|---|---|---|---|---|---|---|
| 0.04 | 0.015 | 0.016 | 20 | 0.0076 | 0.0043 | 26 | 0.0018 | 0.0011 | 18 | 0.091 | 0.10 | 37 | 30 | 12.4 | −9 |
| 0.08 | 0.004 | 0.018 | 22 | 0.0097 | 0.0021 | 30 | 0.0010 | 0.0003 | 20 | 0.031 | 0.16 | 36 | 43 | 12.6 | −11 |
| 0.25 | 0.008 | 0.019 | 21 | 0.0039 | 0.0044 | 27 | 0.0017 | 0.0006 | 18 | 0.030 | 0.20 | 29 | 57 | 12.7 | −14 |
| 1 | 0.055 | 0.034 | 6.7 | < | 0.027 | 33 | 0.0002 | 0.0003 | 24 | 0.042 | 0.13 | 29 | 63 | 12.8 | −8 |
| 2 | 0.19 | 0.0071 | 1.7 | < | 0.041 | 21 | 0.0009 | < | 18 | 0.18 | 0.024 | 39 | 39 | 12.6 | 9 |
| 7 | 0.16 | 0.0031 | 1.3 | < | 0.014 | 12 | 0.0011 | < | 14 | 0.49 | 0.015 | 40 | 18 | 12.2 | 12 |
| 28 | 0.15 | 0.0044 | 2.1 | < | 0.010 | 13 | 0.0009 | < | 16 | 0.42 | 0.020 | 43 | 15 | 12.2 | 20 |
| 56 | 0.17 | 0.0056 | 2.2 | < | 0.0092 | 15 | 0.0005 | < | 19 | 0.31 | 0.022 | 48 | 17 | 12.2 | 17 |
| 209 | 0.19 | 0.0070 | 2.5 | < | 0.010 | 18 | 0.0004 | < | 23 | 0.25 | 0.025 | 50 | 20 | 12.3 | 15 |
| 360 | 0.20 | 0.0017 | 2.8 | 0.0002 | 0.0060 | 19 | 0.0006 | < | 24 | 0.22 | 0.026 | 52 | 19 | 12.3 | – |
| 1310 | 0.38 | 0.0018 | 2.7 | <0.004 | 0.010 | 17 | 0.0011 | <0.003 | 23 | 0.21 | 0.031 | 60 | 21 | 12.2 | 16 |
| Blank | < | < | 0.001 | < | < | < | 0.0001 | < | 0.001 | 0.004 | < | 0.1 | | | |
| DL | 0.001 | 2E−5 | 3E−4 | 2E−4 | 1E−4 | 7E−4 | 4E−5 | 0.0003 | 7E−4 | 0.004 | 3E−6 | 0.008 | | | |

Measurement error ±10%; DL: detection limit. The measured concentrations of Cs are below the DL of 0.2 mM; measured values for Zn ranged from 0.0003 to 0.001 mM.

[a] In the initial mixing solution 370 mM DOC was found; 364 from SP and 6 from cement.

[b] The values for $OH^-$ refer to the free concentration as calculated from the measured pH values.

[c] Charge balance (cb) = (sum(anions) − sum(cations))/(sum anions). sum(cations) = Na + K + 2*Ca; sum(anions) = $OH^-$ + sulfide ($HS^-$) + 2 × (thiosulfate ($S_2O_3^{2-}$) + sulfite ($SO_3^{2-}$) + sulfate ($SO_4^{2-}$)); S species as given in Table 5.

**Table 5**
Measured concentrations of different sulfur species in the pore solution.

| Age [days] | Sulfide | Thiosulfate [mM] | Sulfite | Sulfate | $S_{tot}$ [a] | ($\Delta_S$ [b]) | Acidic "$S_{tot}$" [c] |
|---|---|---|---|---|---|---|---|
| 0.04 | < | 0.29 | < | 22.9 | 25 | (1) | 25 |
| 0.08 | < | 0.34 | < | 20.8 | 23 | (1) | 22 |
| 0.25 | < | 0.46 | < | 9.4 | 10 | (0.0) | 11 |
| 1 | 0.4 | 0.23 | 0.20 | 0.1 | 1.0 | (−0.3) | 0.9 |
| 2 | 5.0 | < | 0.25 | 1.0 | 6.4 | (0.1) | 2.9 |
| 7 | 5.3 | 1.3 | 1.2 | 1.8 | 7.2 | (−4) | 5.4 |
| 28 | 11 | 3.0 | 1.5 | 3.4 | 15 | (−7) | 6.1 |
| 56 | 8.8 | 4.3 | 2.1 | 4.2 | 18 | (−5) | 5.5 |
| 209 | 11 | 4.6 | 2.1 | 4.8 | 22 | (−5) | 9.9 |
| 360 | na | na | na | na | na | 8.4 | |
| 1310 | 8.8 | 4.6 | 1.9 | 6.1 | 22 | (−3) | 4.4 |
| Blank | < | < | < | < | < | < | |
| DL | 0.1 | 0.04 | 0.1 | 0.1 | 0.03 | 0.01 | |

Measurement error ±10%; for sulfide ±20%.
na: not analyzed.
[a] The total concentration of sulfur was determined in alkaline solutions.
[b] $\Delta_S$ = difference between total sulfur measured in alkaline solution and the sum of sulfide + 2 * thiosulfate + sulfite + sulfate.
[c] The measurement of sulfur in acidified solutions (acidic "$S_{tot}$"), results in the loss of $H_2S$ and $SO_2$ from the solutions into the atmosphere, and thus represents only a part of the sulfur content of the solution.

uptake of SP in cements can vary strongly depending on the composition and fineness of the cement and depending on the PCE used. The chain length, chain density, backbone length and the chemistry of the side chains and backbone of the PCE can vary significantly among the different superplasticizers, resulting in a strongly different uptake behavior of the PCE according to their structure (e.g. [87,88]).

### 3.4.2. Saturation indices

Calculation of saturation indices from the concentrations determined in the pore solutions offers the possibility of assessing independently which solid phases can form or will dissolve from a thermodynamic point of view. The saturation index (SI) with respect to a solid is given by $\log(IAP/K_{S0})$, where the ion activity product IAP is calculated from activities derived from the measured concentrations in the solution and $K_{S0}$, which corresponds to the solubility product of the respective solid. A positive saturation index implies oversaturation (the solid can form) while a negative value indicates undersaturation with regard to the respective solid (the solid cannot form or will dissolve). As the use of saturation indices can be misleading when comparing phases which dissociate into a different number of ions, "effective" saturation indices are calculated by dividing the saturation indices by the number of ions participating in the reactions [37,74]. The formation of solids from the dominant ions $OH^-$, $Ca^{2+}$, $SO_4^{2-}$, or $Al(OH)_4^-$ in the solution was considered while the influence of $H_2O$ was neglected. The values for gypsum, portlandite, ettringite, monosulfate, monocarbonate, $C_3AH_6$, jennite or tobermorite were divided by 2, 3, 15, 11, 11, 9, 5 or 3, respectively.

During the first hour, the solutions were saturated or near to saturation with respect to gypsum, portlandite, jennite, ettringite, monosulfate, monocarbonate and hydrotalcite (Fig. 11), comparable to the pore solutions in Portland cement [37,74]. Gypsum was depleted between 2 and 6 h. After 2 days and longer, the pore solutions became strongly undersaturated with respect to portlandite and to a lesser extent also with respect to jennite-like C-S-H, indicating the reaction of the silica rich nanosilica and slag. After 2 days and longer the solutions were oversaturated with respect to pyrite ($FeS_2$) and troilite (FeS), but undersaturated with respect to the more disordered mackinawite (FeS). After 1 week and longer, the pore solutions became saturated with respect to ettringite, hydrotalcite, tobermorite-like C-S-H and strätlingite, while they remained undersaturated with respect to hydrogarnet ($C_3AH_6$). After the first day the solutions were slightly undersaturated with respect to monocarbonate and monosulfate.

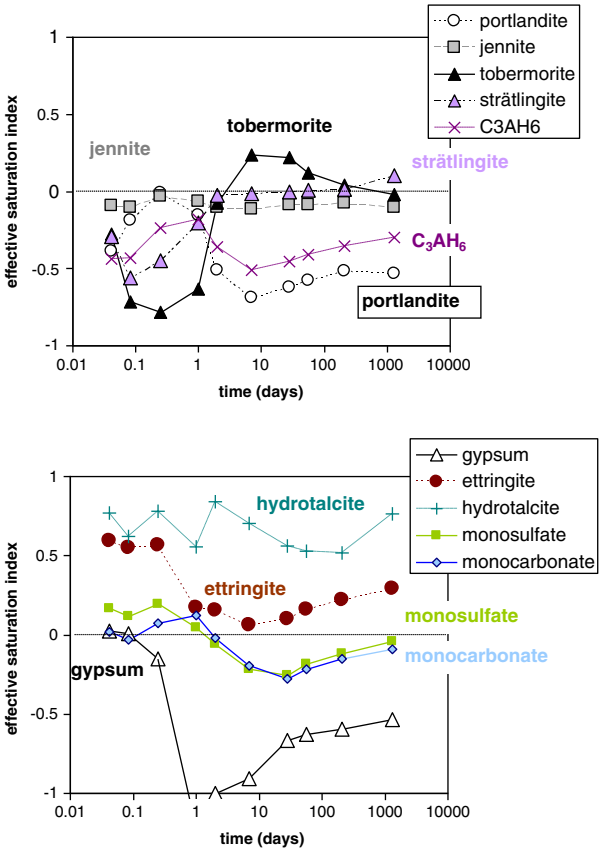


**Fig. 11.** Calculated effective saturation indices as a function of hydration time. A saturation index of 0 indicates equilibrium.

Thus, the saturation indices indicate the presence of tobermorite-like C-S-H, ettringite, hydrotalcite, FeS and strätlingite, which is consistent with experimental findings from solid phase analysis except for strätlingite and FeS whose presence is indicated by the SI only.

Note that the saturation indices indicate the possible formation of thaumasite (eff. SI ~ 0.2) and Si-hydrogarnet (eff. SI ~ 0.5). As discussed previously, small amounts of Al/Fe containing Si-hydrogarnet had been observed after prolonged hydration at ambient temperatures in Portland cements [37,70 — 73,89] and may not form at ambient temperatures in the absence of Fe(III) [90]. The formation of thaumasite is kinetically hindered at room temperature. The positive saturation indices for thaumasite, however, could indicate the possible presence of a small quantity of thaumasite in a solid solution with ettringite.

## 4. Thermodynamic modeling

### 4.1. Modeling of hydration

Thermodynamic modeling of the hydration of LAC was carried out in a fashion similar to that described earlier for Portland cements [3,37,48]. The kind and amount of hydrates formed was calculated by combining an empirical model that describes the dissolution of the clinker phases as a function of time [91] with a thermodynamic equilibrium model that assumes equilibrium between the solution and the hydrates [3,37,48]. The mixing proportions and the mineralogical composition as reported in Table 1 were used as input data.

#### 4.1.1. Dissolution of clinker phases, slag and nanosilica

The reaction of the different clinker phases in PC, slag and the 10 wt.% $SiO_2$ occurs simultaneously at different rates. The dissolution of the clinker phases as a function of time was estimated using the

empirical kinetic approach of Parrot and Killoh [91] and the parameters given elsewhere [37]. This approach somewhat underestimates the experimentally observed degree of clinker reaction during the first days (Fig. 12A), as the presence of the slag and nanosilica increased the degree of reaction of the clinker phases due to the filler effect [24,64,92].

The reaction of the slag and the nanosilica was described using the following empirical equations fitted to the experimentally determined data:

$$\text{unreacted slag [in g/100 g]} = 0.59 * (100 - 37 - 18.5 * \log(\text{time}))$$
(for 0.01 day ≤ time ≤ 2400 days)

$$\text{unreacted nanosilica} = 10 \times 10^{-0.25 * (\text{time})}$$ (time in [days])

which describes the measured data well (Fig. 12).

*4.1.2. Calculated hydrate assemblage*

Thermodynamic modeling, using the dissolution kinetics derived above, predicts the formation of C-S-H with Ca/Si ratio of ~1.1, ettringite, hydrotalcite and strätlingite as well as traces of FeS (troilite) (Fig. 13). The presence of low Ca/Si C-S-H, ettringite and calcite and the absence of portlandite agrees well with the experimental XRD,

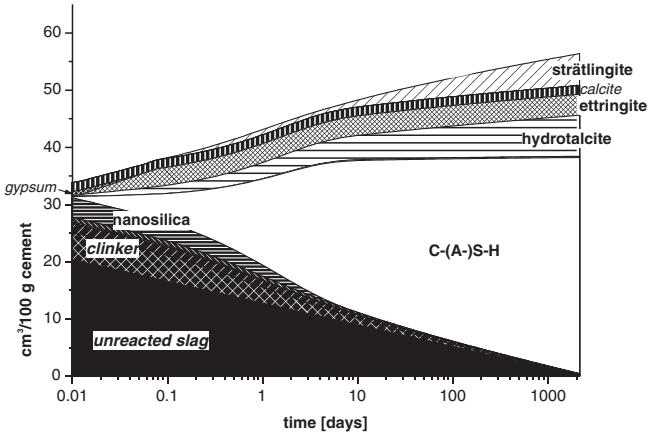


**Fig. 13.** Modeled changes during the hydration of LAC expressed as volume ($cm^3$/100 g unhydrated cement). The uptake of aluminum by the C-S-H was taken into account using the measured Al/Si ratio (=0.12).

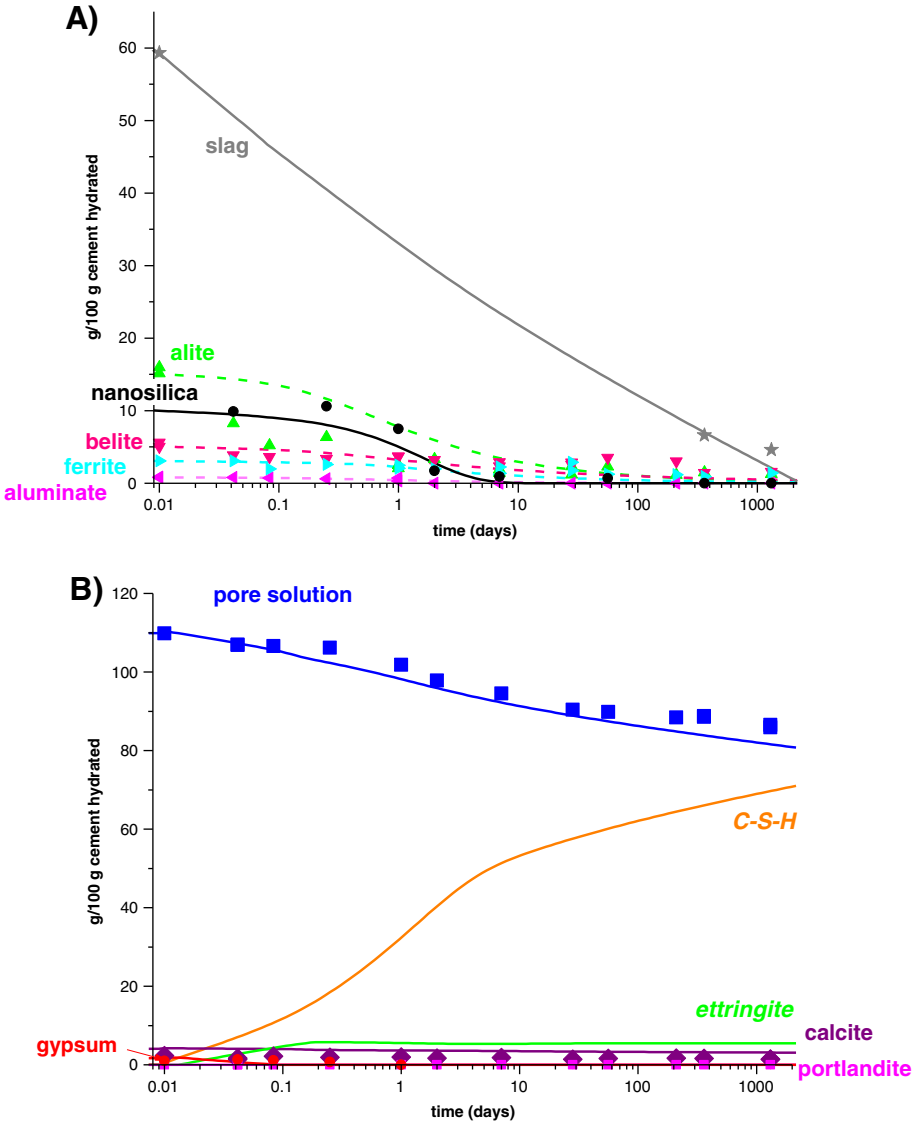


**Fig. 12.** A) Semi quantitative evaluation of the XRD patterns and the measured amount of slag and nanosilica after different hydration times (symbols) compared with modeled clinker, slag and nanosilica dissolution (lines). B) Comparison of the amount of portlandite, calcite, gypsum and pore solution determined by TGA measurements with the modeled amount.

TGA and NMR results (see Figs. 3, 5, 6 and 12B). Hydrotalcite and strätlingite have not been identified by XRD, but TGA and SEM/EDX indicate the presence of hydrotalcite and the pore solutions are oversaturated with respect to strätlingite (Fig. 11) and FeS. The latter findings confirm indirectly the presence of strätlingite and FeS. In contrast to the experimental observations, however, the presence of hemi- or monocarbonate is not predicted while small amounts of hemicarbonate were observed by XRD between 1 day and 1 year. After 3.5 years, however, hemicarbonate had disappeared, and only ettringite and C-S-H were identified, which agrees with the model predictions. The uptake of Al by C-S-H could not be modeled instead the measured Al/Si ratio of 0.12 was used in the calculations. When the uptake of Al by C-S-H was neglected in the calculations, a similar phase composition resulted with the only difference that less C-S-H but more strätlingite formed.

The composition of the liquid phase could not be predicted satisfactorily due to the lack of thermodynamic models for Al uptake in C-S-H, the lack of information on $O_2$ ingress during the experiments and the kinetic of the sulfur redox reactions. However, even though we are not yet able to predict the composition of the pore solution adequately, the saturation indices calculated on the basis of the concentrations measured in the pore solution agree well with the solid phase assemblage.

In the absence of $O_2$ ingress, the thermodynamic modeling predicts that the iron present in the clinker was reduced from Fe(+III) to Fe(+II), while a portion of the sulfide (S(−II)) was oxidized to sulfate (S(+VI)). The presence of reduced Fe is supported by the increased Fe-concentrations measured in the pore solution, as Fe(II) species are more soluble at high pH values than Fe(III). If $O_2$ could ingress, more S(−II) from the slag would oxidize to sulfate resulting in the formation of larger amounts of ettringite.

### 4.2. Influence of the reactivity of the slag

The slag in LAC reacted more slowly than the nanosilica and the clinker minerals. After 1 month about 2/3 and after 3.5 years about 90% of the slag initially present had reacted. Thermodynamic modeling was used to calculate the changes associated with the reaction of the slag (Fig. 14).

Even if no slag had reacted, the presence of 10% nanosilica has a strong impact on the calculated phase assemblage (left side of Fig. 14A and B). The presence of nanosilica leads to complete depletion of the portlandite as only 31 g PC/100 g LAC was present (Fig. 14A). In the absence of $SiO_2$, the presence of C-S-H with high Ca/Si, portlandite, ettringite, hydrotalcite and monocarbonate was calculated (Fig. 14B).

The reaction of the slag in LAC gives rise to the formation of strätlingite, and increasing amounts of C-S-H and hydrotalcite as shown in Fig. 14A. The calculated pH value ranges from 12.5 to 13 and is not strongly affected by the reaction of the slag. The calculations predicted no significant changes in the phase composition of LAC between one month and 3.5 years of hydration, which is consistent with the experimental findings. According to the calculations no significant changes are expected to occur with ongoing hydration unless the samples would oxidize or Si-hydrogarnet would form (see discussion below).

For the CEM III/B cement (Fig. 14B), in the absence of additional $SiO_2$, portlandite was calculated to be consumed upon the reaction of the slag, while the amount of ettringite remained more or less constant. The amount of hydrotalcite, monocarbonate and tobermorite-like C-S-H was increased compared to LAC. The complete consumption of portlandite was predicted to occur only at relatively high slag contents and at high degree of slag reaction [9]. At lower slag contents, experimental evidence showed that portlandite persisted for many years [14,15] as slags are relatively CaO rich and as the Ca/Si ratio of C-S-H decreases in PC–slag blends even in the presence of portlandite [14,15]. Note that such a decrease in the Ca/Si ratio in the presence of portlandite is not captured by the present thermodynamic model.

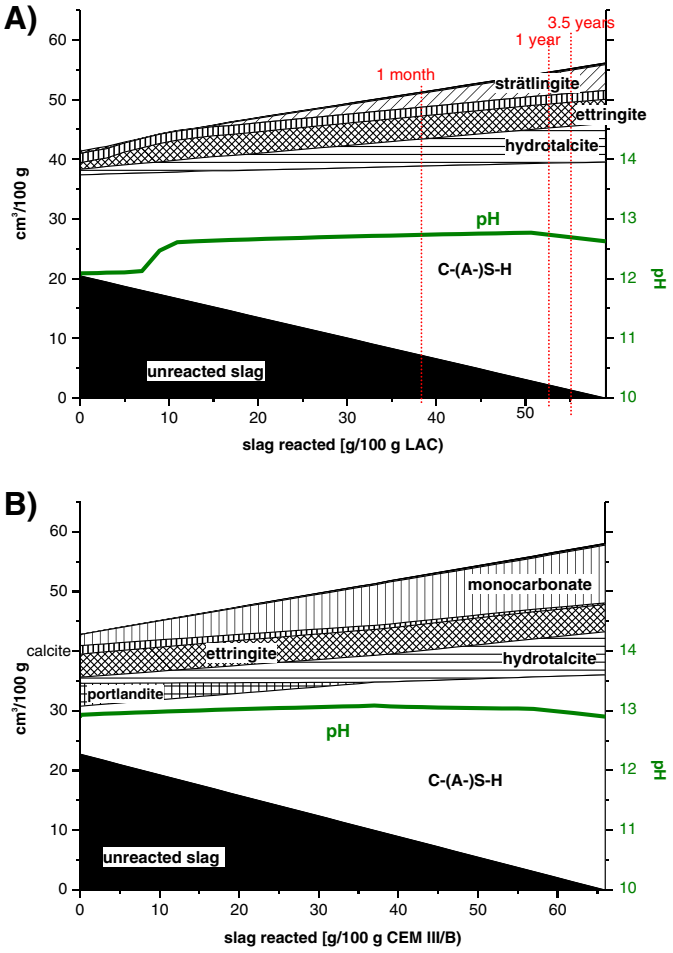


**Fig. 14.** Modeled changes caused by the reaction of the slag in A) LAC cement (10% NS, 59% slag, 31 PC) and B) CEM III/B (66% slag, 34 PC). Volume in $cm^3$/100 g unhydrated cement.

### 4.3. Long-term development

In the calculations shown above the formation of Si-hydrogarnet has been excluded for kinetic reasons. Possible changes in the solid phase composition in the timeframe from 1000 to 10,000 of years are of importance in connection with the disposal of radioactive waste. In archeological binders, the presence of calcite, ettringite, C-S-H and Si-hydrogarnet was observed [93]. The ettringite present in such archeological binders was reported to contain some Si and to be deficient in sulfate [93], which could indicate that thaumasite is present. The composition of these ancient binders — C-S-H with Ca/Si ratio of approx. 1 and absence of portlandite — corresponds rather to a low pH cement than to a Portland cement. The C-S-H found in such ancient binders (including very old samples from Hadrian's wall and from Gallo-Roman baths) was similar to C-S-H found in modern cements with an equivalent Ca/Si ratio. C-S-H aged for approximately 1900 years was still X-ray amorphous [93–96] and had not converted into more crystalline solids such as tobermorite or xonotlite. This suggests that the kinetics of the corresponding conversion reactions must be very slow.

Additional calculations were carried out to study the possible long-term development of the LAC by assuming complete hydration of PC–slag blend (Fig. 15). The first column in Fig. 15 corresponds to the data shown in Fig. 13 after long hydration times as it was assumed

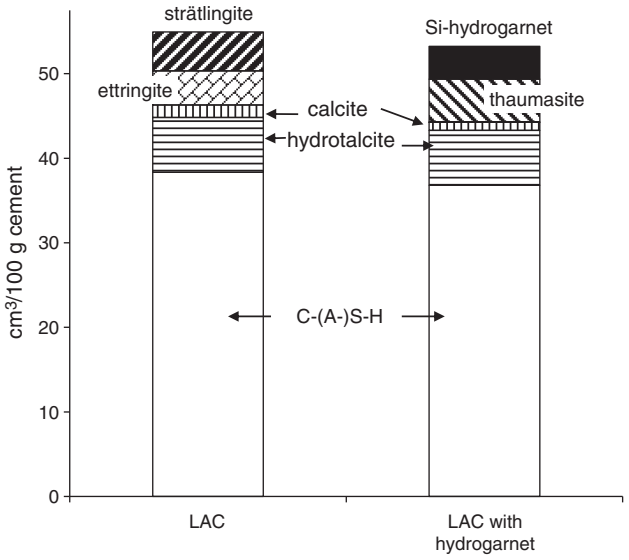


**Fig. 15.** Modeled composition of completely hydrated LAC expressed as $cm^3/100$ g unhydrated cement.

that Si-hydrogarnet cannot form for kinetic reasons. In the second calculation, however, Si-hydrogarnet was allowed to form. About 10 vol.% of Si-hydrogarnet is expected to form while strätlingite becomes unstable (Fig. 15). If Si-hydrogarnet is present, also thaumasite becomes more stable than ettringite. However, to which extent thaumasite or Si-hydrogarnet may form in the long term is currently uncertain. After 3.5 year hydration neither thaumasite nor Si-hydrogarnet were observed experimentally in this study. A possible explanation could be that only Fe(III)-containing Si-hydrogarnet can form at room temperature, while in the hydrated LAC the major portion of iron was probably reduced to Fe(II).

## 5. Conclusions

The LAC mixture investigated in this study consists of a CEM III/B 42.5 L-LH HS mixed with 10 wt.% nanosilica (>99.8 $SiO_2$), resulting in a blend with 31 wt.% Portland cement, 59 wt.% slag and 10 wt.% $SiO_2$. The reaction of all these solids occurs simultaneously at different rates. The nanosilica is completely consumed after a few days, while 90% of the slag has reacted after 3.5 year hydration. The experimentally observed phase assemblage consists of C-(A-)S-H (Ca/Si = 1.2) with significant incorporation of aluminum, hydrotalcite, ettringite, strätlingite and some calcite. The pore solution is dominated by sodium, potassium, hydroxide, and by different sulfur species, mainly $HS^-$ but also $SO_4^{2-}$, $S_2O_3^{2-}$ and $SO_3^{2-}$, indicating reducing conditions due to the reaction of the slag. The alkali concentrations (K + Na: ~40 mM) are ten times lower than in Portland cements as in the LAC three times less Portland cement is present and as the low Ca/Si C-S-H formed takes up the alkalis efficiently. The presence of 20 mM negatively charged sulfur species reduces the concentration of hydroxides in the pore solutions, thus lowering the pH. After 3.5 years a pH value of 12.2 results, which is much lower than the pH of 13.5–13.8 reported for Portland cements [2,3,37,97].

Between 1 month and 3.5 years no significant differences in the composition of the pore solution and the solid phase assemblage have been observed. Nevertheless, an increase in the amount of hydrates occurs due to the reaction of the slag during this period of time. Thermodynamic modeling predicts the presence of C-S-H with a Ca/Si of 1, ettringite, hydrotalcite, calcite and strätlingite. The calculated changes of the amount of hydrates are relatively small after the first month, in agreement with the experimental observations.

The 10% nanosilica present and the low amount of Portland cement in the LAC are responsible for the absence of portlandite and the relatively low pH value of 12.2, while the reaction of the slag gives rise to reducing conditions and the formation of more hydrotalcite and possibly strätlingite.

It should be noted that the thermodynamic calculations suggest the formation of Si-hydrogarnet in the long term and, in the presence of Si-hydrogarnet, of thaumasite. However, even after 3.5 year hydration neither Si-hydrogarnet nor thaumasite could be detected, indicating that the kinetics of formation of these cement minerals is very slow in the LAC possibly due to absence of Fe(III) under the reducing conditions of this slag containing blend.

## Acknowledgments

The partial financial support from the Cement Clay Interaction (CI) project at Mont Terri is gratefully acknowledged. The authors would like to thank Angela Steffen, Luigi Brunetti, Boris Ingold and Dominik Kunz for carrying out the laboratory experiments, Martin Glaus for the DOC analysis, Daniel Rentsch for the $^{29}Si$ MAS NMR measurements, Oliver Nagel for analytical services and Frank Winnefeld, Ken Snyder, Urs Mäder and Bernhard Schwyn for helpful discussions.

## References

[1] N. Chapman, C. McCombie, Principles and Standards for the Disposal of Long-lived Radioactive Wastes, 1 ed. Oxford Elsevier Science Ltd., 2003.
[2] D. Rothstein, J.J. Thomas, B.J. Christensen, H.M. Jennings, Solubility behavior of Ca-, S-, Al-, and Si-bearing solid phases in Portland cement pore solutions as a function of hydration time, Cem. Concr. Res. 32 (10) (2002) 1663–1671.
[3] B. Lothenbach, F. Winnefeld, Thermodynamic modelling of the hydration of Portland cement, Cem. Concr. Res. 36 (2) (2006) 209–226.
[4] M. Codina, C. Cau-dit-Coumes, P. Le Bescop, J. Verdier, J.P. Ollivier, Design and characterization of low heat and low-alkalinity cements, Cem. Concr. Res. 38 (2008) 437–448.
[5] J.L. Garcia Calvo, A. Hidalgo, C. Alonso, L. Fernandez Luco, Development of low-pH cementitious materials for HLRW repositories. Resistance against ground waters aggression, Cem. Concr. Res. 40 (8) (2010) 1290–1297.
[6] C. Cau-dit-Coumes, S. Courtois, D. Nectoux, S. Leclercq, X. Bourbon, Formulating a low-alkalinity, high resistance and low-heat concrete for radioactive waste repositories, Cem. Concr. Res. 36 (2006) 2152–2163.
[7] B. Lothenbach, D. Rentsch, E. Wieland, Hydration of a CEM I-$SiO_2$ based low-alkali shotcrete cement (ESRDED). Cem. Concr. Compos. (submitted for publication).
[8] H.F.W. Taylor, Cement Chemistry, Thomas Telford Publishing, London, 1997.
[9] B. Lothenbach, K. Scrivener, R.D. Hooton, Supplementary cementitious materials. Cem. Concr. Res. 41 (12) (2011) 1244–1256.
[10] V. Kocaba, Development and evaluation of methods to follow microstructural development of cementitious systems including slags. Thesis EPFL No 4523, Lausanne, Switzerland: 263pp. (2009).
[11] E. Schäfer, Einfluss der Reaktion verschiedener Zementhauptbestandteile auf den Alkalihaushalt der Porenlösung des Zementsteins, 179, Verlag Bau + Technik GmbH, Düsseldorf, Germany, 2006.
[12] F.P. Glasser, M. Tyrer, K. Quillin, D. Ross, J. Pedersen, K. Goldthorpe, D.G. Bennett, M. Atkins, The chemistry of blended cements and backfills intended for use in radioactive waste disposal, UK Environment Agency Technical Report, P98, 1998.
[13] J.I. Escalante-Garcia, J.H. Sharp, The chemical composition and microstructure of hydration products in blended cements, Cem. Concr. Compos. 26 (2004) 967–976.
[14] K. Luke, E. Lachowski, Internal composition of 20-year-old fly ash and slag-blended ordinary Portland cement pastes, J. Am. Ceram. Soc. 91 (12) (2008) 4084–4092.
[15] R. Taylor, I.G. Richardson, R.M.D. Brydson, Composition and microstructure of 20-year-old ordinary Portland cement-ground granulated blast-furnace slag blends containing 0 to 100% slag, Cem. Concr. Res. 40 (7) (2010) 971–983.
[16] A.M. Harrisson, N.B. Winter, H.F.W. Taylor, An examination of some pure and composite Portland cement pastes using scanning electron microscopy with X-ray analytical capability, 8th ICCC, 4, 1986, pp. 170–175.
[17] J.I. Escalante-Garcia, L.Y. Gomez, K.K. Johal, G. Mendoza, H. Mancha, J. Méndez, Reactivity of blast-furnace slag in Portland cement blends hydrated under different conditions, Cem. Concr. Res. 31 (2001) 1403–1409.
[18] I. Pane, W. Hansen, Investigation of blended cement hydration by isothermal calorimetry and thermal analysis, Cem. Concr. Res. 35 (2005) 1155–1164.
[19] I.G. Richardson, G.W. Groves, The structure of the calcium silicate hydrate phases present in hardened pastes of white Portland cement blast-furnace slag blends, J. Mater. Sci. 32 (18) (1997) 4793–4802.
[20] I.G. Richardson, The nature of C-S-H in hardened cements, Cem. Concr. Res. 29 (8) (1999) 1131–1147.

[21] M. Atkins, F.P. Glasser, A. Kindness, Phase relation and solubility modelling in the $CaO–SiO_2–Al_2O_3–MgO–SO_3–H_2O$ system: for application to blended cements, Mater. Res. Soc. Symp. Proc. 212 (1991) 387–394.
[22] H. Cheng-yi, R.F. Feldman, Hydration reactions in Portland cement-silica fume blends, Cem. Concr. Res. 15 (1985) 585–592.
[23] B.W. Langan, K. Weng, M.A. Ward, Effect of silica fume and fly ash on heat of hydration of Portland cement, Cem. Concr. Res. 32 (2002) 1045–1051.
[24] S.L. Poulsen, H.J. Jakobsen, J. Skibsted, Methodologies for measuring the degree of reaction in Portland cement blends with supplementary cementitious materials by $^{27}Al$ and $^{29}Si$ MAS NMR spectroscopy. 17, Volume 1, Internationale Baustofftagung (ibausil), Weimar, Germany, 2009, pp. 177–188.
[25] H. Cheng-yi, R.F. Feldman, Influence of silica fume on the microstructural development in cement mortars, Cem. Concr. Res. 15 (1985) 285–294.
[26] P.J.M. Monteiro, O.E. Gjorv, P.K. Mehta, Effect of condensed silica fume on the steel–cement paste transition zone, Cem. Concr. Res. 19 (1989) 114–123.
[27] J. Duchesne, M.A. Bérubé, Evaluation of the validity of the pore solution expression method from hardened cement pastes and mortars, Cem. Concr. Res. 24 (3) (1994) 456–462.
[28] Rasheeduzzafar, E.S. Hussain, Effect of microsilica and blast furnace slag on pore solution composition and alkali–silica reaction, Cem. Concr. Compos. 13 (1991) 219–225.
[29] F.P. Glasser, K. Luke, M.J. Angus, Modification of cement pore fluid compositions by pozzolanic additives, Cem. Concr. Res. 18 (2) (1988) 165–178.
[30] S.-Y. Hong, F.P. Glasser, Alkali binding in cement pastes. Part I. The C-S-H phase, Cem. Concr. Res. 29 (1999) 1893–1903.
[31] H. Stade, On the reaction of C-S-H(di, poly) with alkali hydroxides, Cem. Concr. Res. 19 (1989) 802–810.
[32] J. Duchesne, M.A. Bérubé, The effectiveness of supplementary cementing materials in suppressing expansion due to ASR: another look at the reaction mechanisms. Part 2: pore solution chemistry, Cem. Concr. Res. 24 (2) (1994) 221–230.
[33] A. Franke, Bestimmung von Calciumoxid und Calciumhydroxid neben wasserfreiem und wasserhaltigem Calciumsilikat, Z. Anorg. Allg. Chem. 247 (1941) 180–184.
[34] P. Gunkel, K. Hallich, K. Lesch, W. Lieber, H. Otterbein, H. Pisters, W. Rechenberg, A. Sassenscheidt, H. Zeeh, Analysengang für Zemente, Beton-Verlag GmbH, Düsseldorf, Germany, 1970.
[35] G. Le Saout, V. Kocaba, K.L. Scrivener, Application of the Rietveld method to the analysis of anhydrous cement, Cem. Concr. Res. 41 (2) (2011) 133–148.
[36] G. Le Saout, E. Lécolier, A. Rivereau, H. Zanni, Chemical structure of cement aged at normal and elevated temperatures and pressures. Part I. Class G oilwell cement, Cem. Concr. Res. 36 (1) (2006) 71–78.
[37] B. Lothenbach, G. Le Saout, E. Gallucci, K. Scrivener, Influence of limestone on the hydration of Portland cements, Cem. Concr. Res. 38 (6) (2008) 848–860.
[38] D. Massiot, et al., Modelling one- and two-dimensional solid-state NMR spectra, Magn. Reson. Chem. 40 (2002) 70–76.
[39] M. Ben Haha, E. Gallucci, A. Guidoum, K.L. Scrivener, Relation of expansion due to alkali silica reaction to the degree of reaction measured by SEM image analysis, Cem. Concr. Res. 37 (8) (2007) 1206–1214.
[40] M. Ben Haha, K. De Weerdt, B. Lothenbach, Quantification of the degree of reaction of fly ash, Cem. Concr. Res. 40 (11) (2010) 1620–1629.
[41] K.L. Scrivener, Backscattered electron imaging of cementitious microstructures: understanding and quantification, Cem. Concr. Compos. 26 (8) (2004) 935–945.
[42] J.S. Lumley, R.S. Gollop, G.K. Moir, H.F.W. Taylor, Degrees of reaction of the slag in some blends with Portland cement, Cem. Concr. Res. 26 (1) (1996) 139–151.
[43] A. Gruskovnjak, B. Lothenbach, L. Holzer, R. Figi, F. Winnefeld, Hydration of alkali-activated slag: comparison with ordinary Portland cement, Adv. Cem. Res. 18 (3) (2006) 119–128.
[44] D. Kulik, GEMS-PSI 3, PSI-Villigen, Switzerland, 2010 available at, http://gems.web.psi.ch/.
[45] D. Kulik, U. Berner, E. Curti, Modelling Geochemcial Equilibrium Partitioning with the GEMS-PSI Code, , 2004.
[46] T. Thoenen, D. Kulik, Nagra/PSI chemical thermodynamic database 01/01 for the GEM-Selektor (V.2-PSI) geochemical modeling code, PSI TM-44-02-09, 2003.
[47] W. Hummel, U. Berner, E. Curti, F.J. Pearson, T. Thoenen, Nagra/PSI Chemical Thermodynamic Data Base 01/01, USA, also published as Nagra Technical Report NTB 02–16, 565, Universal Publishers/uPUBLISH.com, Wettingen, Switzerland, 2002.
[48] B. Lothenbach, T. Matschei, G. Möschner, F.P. Glasser, Thermodynamic modelling of the effect of temperature on the hydration and porosity of Portland cement, Cem. Concr. Res. 38 (1) (2008) 1–18.
[49] T. Matschei, B. Lothenbach, F.P. Glasser, Thermodynamic properties of Portland cement hydrates in the system $CaO–Al_2O_3–SiO_2–CaSO_4–CaCO_3–H_2O$, Cem. Concr. Res. 37 (10) (2007) 1379–1410.
[50] T. Schmidt, B. Lothenbach, M. Romer, K.L. Scrivener, D. Rentsch, R. Figi, A thermodynamic and experimental study of the conditions of thaumasite formation, Cem. Concr. Res. 38 (3) (2008) 337–349.
[51] D.E. Macphee, S.J. Barnett, Solution properties of solids in the ettringite–thaumasite solid solution series, Cem. Concr. Res. 34 (2004) 1591–1598.
[52] D.A. Kulik, M. Kersten, Aqueous solubility diagrams for cementitious waste stabilization systems: 4. A carbonation model for Zn-doped calcium-silicate hydrate by Gibbs energy minimization, Environ. Sci. Technol. 36 (2002) 2926–2931.
[53] D.A. Kulik, M. Kersten, Aqueous solubility diagrams for cementitious waste stabilization systems: II. End-member stoichiometries of ideal calcium silicates hydrate solid solutions, J. Am. Ceram. Soc. 84 (12) (2001) 3017–3026.
[54] I.G. Richardson, A. Brough, R. Brydson, G.W. Groves, C.M. Dobson, Location of aluminum in substituted calcium silicate hydrate (C-S-H) gels as determined by $^{29}Si$ and $^{27}Al$ NMR and EELS, J. Am. Ceram. Soc. 79 (6) (1993) 2285–2288.
[55] G. Renaudin, J. Russias, F. Leroux, F. Frizon, C. Cau-dit-Coumes, Structural characterization of C-S-H and C-A-S-H samples — Part I: long-range order investigated by Rietveld analyses, J. Solid State Chem. 182 (2009) 3312–3319.
[56] P. Yu, R.J. Kirkpatrick, B. Poe, P.F. McMillan, X. Cong, Structure of calcium silicate hydrate (C-S-H): near-, mid-, and far-infrared spectroscopy, J. Am. Ceram. Soc. 82 (3) (1999) 742–748.
[57] D. Kulik, J. Tits, E. Wieland, Aqueous-solid solution model of strontium uptake in C-S-H phases, Geochim. Cosmochim. Acta 71 (12, Supplement 1) (2007) A530.
[58] M. Wolthers, L. Charlet, P.R. Van der Linde, D. Rickard, C.H. Van der Weijden, Surface chemistry of disordered mackinawite (FeS), Geochim. Cosmochim. Acta 69 (14) (2005) 3469–3481.
[59] V.I. Babushkin, G.M. Matveyev, O.P. Mchedlov-Petrossyan, Thermodynamics of Silicates, 459, Springer-Verlag, Berlin, 1985.
[60] J. Hjorth, J. Skibsted, H.J. Jakobsen, 29Si MAS NMR studies of Portland cement components and effects of microsilica on the hydration reaction, Cem. Concr. Res. 18 (1988) 789–798.
[61] K. Luke, F.P. Glasser, Selective dissolution of hydrated blast furnace slag cements, Cem. Concr. Res. 17 (2) (1987) 273–282.
[62] H.M. Dyson, I.G. Richardson, A. Brough, A combined $^{29}Si$ NMR and selective dissolution technique for the quantitative evaluation of hydrated blast furnace slag cement blends, J. Am. Ceram. Soc. 90 (2007) 598–602.
[63] A. Gruskovnjak, B. Lothenbach, F. Winnefeld, B. Münch, S.C. Ko, M. Adler, U. Mäder, Quantification of hydration phases in super sulphated cements: review and new approaches, Adv. Cem. Res. 23 (6) (2011) 265–275.
[64] V. Kocaba, E. Gallucci, K. Scrivener, Methods for determination of degree of reaction of slag in blended cement pastes. Cem. Concr. Res. (submitted for publication).
[65] G. Le Saout, M. Ben Haha, F. Winnefeld, B. Lothenbach, Hydration degree of alkali activated slags, J. Am. Ceram. Soc. 94 (12) (2011) 4541–4547.
[66] S.-D. Wang, K.L. Scrivener, $^{29}Si$ and $^{27}Al$ NMR study of alkali-activated slag, Cem. Concr. Res. 33 (5) (2003) 769–774.
[67] G.M. Bell, J. Bensted, F.P. Glasser, E.E. Lachowski, D.R. Roberts, M.J. Taylor, Study of calcium silicate hydrates by solid state high resolution $^{29}Si$ nuclear magnetic resonance, Adv. Cem. Res. 3 (1) (1990) 23–37.
[68] M. Ben Haha, G. Le Saout, F. Winnefeld, B. Lothenbach, Influence of slag chemistry on the hydration of alkali activated blast-furnace slag — Part I: effect of $Al_2O_3$, Cem. Concr. Res. 42 (1) (2012) 74–83.
[69] H.F.W. Taylor, D.E. Newbury, An electron microprobe study of a mature cement paste, Cem. Concr. Res. 14 (4) (1984) 565–573.
[70] R.S. Gollop, H.F.W. Taylor, Microstructural and microanalytical studies of sulfate attack. II. Sulfate-resisting Portland cement: ferrite composition and hydration chemistry, Cem. Concr. Res. 24 (7) (1994) 1347–1358.
[71] M. Paul, F.P. Glasser, Impact of prolonged warm (85 degrees C) moist cure on Portland cement paste, Cem. Concr. Res. 30 (12) (2000) 1869–1877.
[72] B. Lothenbach, E. Wieland, A thermodynamic approach to the hydration of sulphate-resisting Portland cement, Waste Manage. 26 (7) (2006) 706–719.
[73] B.Z. Dilnesa, B. Lothenbach, G. Le Saout, E. Wieland, K.L. Scrivener, Fe-containing hydrates in cementitious systems, ICCC, 2011 Madrid, 2011, article no 211, 7pp.
[74] B. Lothenbach, Thermodynamic equilibrium calculations in cementitious systems, Mater. Struct. 43 (2010) 1413–1433.
[75] B. Lothenbach, F. Winnefeld, C. Alder, E. Wieland, P. Lunk, Effect of temperature on the pore solution, microstructure and hydration products of Portland cement pastes, Cem. Concr. Res. 37 (4) (2007) 483–491.
[76] G. Möschner, B. Lothenbach, R. Figi, R. Kretschmar, Influence of citric acid on the hydration of Portland cement, Cem. Concr. Res. 39 (4) (2009) 275–282.
[77] K.Y. Chen, J.C. Morris, Kinetics of oxidation of aqueous sulfide by $O_2$, Environ. Sci. Technol. 6 (6) (1972) 529–536.
[78] H. Fischer, G. Schulz-Ekloff, D. Wöhrle, Oxidation of aqueous sulfide solutions by dioxygen. Part I: autooxidation reaction, Chem. Eng. Technol. 20 (7) (1997) 462–468.
[79] C. Vernet, Comportement de l'ion S- au cours de l'hydratation des ciments riche en laitier (CLK), Silic. Ind. 47 (1982) 85–89.
[80] A. Gruskovnjak, B. Lothenbach, F. Winnefeld, R. Figi, S.C. Ko, M. Adler, U. Mäder, Hydration mechanisms of supersulphated slag cement, Cem. Concr. Res. 38 (2008) 983–992.
[81] P. Longuet, L. Burglen, A. Zelwer, La phase liquide du ciment hydraté, Revue des matériaux de construction 676 (1973) 35–41.
[82] C. Vernet, E. Démoulian, P. Gourdin, F. Hawthorn, Kinetics of slag cements hydration, 7th International Congress on the Chemistry of Cement, III, 1980, pp. 128–133.
[83] T. Matschei, F. Bellmann, J. Stark, Hydration behaviour of sulphate-activated slag cements, Adv. Cem. Res. 17 (4) (2005) 167–178.
[84] M. Andersson, H. Ervanne, M. Glaus, S. Holgersson, P. Larttunen, H. Laine, B. Lothenbach, I. Puigdomenech, B. Schwyn, M. Snellman, H. Ueda, M. Vuorio, E. Wieland, T. Yamamoto, Development of methodology for evaluation of long-term safety aspects of organic cement paste components, Posiva Working Report 2008-28, 2008.
[85] B. Lothenbach, CI experiment: hydration experiments on OPC, LAC and ESDRED cements: 1 h to 3.5 years, Nagra Technical Note TN 2010-75, 2010.
[86] B. Lothenbach, F. Winnefeld, R. Figi, The influence of superplasticizers on the hydration of Portland cement, 12th International Congress on the Chemistry of Cement. Montreal, Canada, 2007 W1-5.03.
[87] F. Winnefeld, S. Becker, J. Pakusch, T. Götz, Effects of the molecular architecture of comb-shaped superplasticizers on their performance in cementitious systems, Cem. Concr. Compos. 29 (2007) 251–262.

[88] K. Yamada, T. Takahashi, S. Hanehara, M. Matsuhisa, Effects of the chemical structure on the properties of polycarboxylate-type superplasticizer, Cem. Concr. Res. 30 (2) (2000) 197–207.
[89] H.F.W. Taylor, D.E. Newbury, An electron microporbe study of a mature cement paste, Cem. Concr. Res. 14 (1984) 565–573.
[90] B.Z. Dilnesa, personal communication, 2011.
[91] L.J. Parrot, D.C. Killoh, Prediction of cement hydration, Br. Ceram. Proc. 35 (1984) 41–53.
[92] X. Feng, E.J. Garboczi, D.P. Bentz, P.E. Stutzman, T.O. Mason, Estimation of the degree of hydration of blended cement pastes by a scanning electron microscope point-counting procedure, Cem. Concr. Res. 34 (10) (2004) 1787–1793.
[93] F. Rassineux, J.C. Petit, A. Meunier, Ancient analogues of modern cement: calcium hydrosilicates in mortar and concrete from Gallo-roman baths of Western France, J. Am. Ceram. Soc. 72 (6) (1989) 1026–1032.
[94] J.C. Petit, Natural analogues for the design and performance assessment of radioactive waste forms: a review, J. Geochem. Explor. 46 (1992) 1–33.
[95] J.A. Staedman, Archaeological conretes as analogues, 2nd Meeting of CEC Analogues Working Group. Interlaken, Switzerland, 1986 Report No EUR 10671 EN.
[96] D.L. Rayment, K. Pettifer, Examination of durable mortar from Hadrain's Wall, Mater. Sci. Technol. 3 (12) (1997) 997–1004.
[97] K. De Weerdt, M. Ben Haha, G. Le Saout, K.O. Kjellsen, H. Justness, B. Lothenbach, Hydration mechanisms of ternary Portland cements containing limestone powder and fly ash, Cem. Concr. Res. 41 (3) (2011) 279–291.